

Supporting Information

Influence of emission bandwidth by charge transfer strength for the multiple resonance emitters via systematically tuning the electron acceptor-donor assembly

Jing-Wei Huang^{1#}, Yu-Chieh Hsu^{2#}, Xiugang Wu^{1#}, Sai Wang¹, Xiang-Qin Gan¹, Wei-Qiong Zheng¹, Hu Zhang¹, Yin-Zhi Gong¹, Wen-Yi Hung^{3*}, Pi-Tai Chou^{2*}, and Weiguo Zhu^{1*}*

¹School of Materials Science and Engineering, Jiangsu Collaboration Innovation Center of Photovoltaic Science and Engineering, Jiangsu Engineering Laboratory of Light-Electricity-Heat Energy-Converting Materials and Applications, National Experimental Demonstration Center for Materials Science and Engineering, Changzhou University, Changzhou 213164, China. E-mail: xgwu16@126.com, zhuwg18@126.com.

²Department of Chemistry, National Taiwan University, Taipei, 10617, Taiwan. E-mail: chop@ntu.edu.tw.

³Department of Optoelectronics and Materials Technology, National Taiwan Ocean University, Keelung, Taiwan. E-mail: wenhung@mail.ntou.edu.tw.

General information

Materials were purchased from commercial suppliers, and were used after appropriate purification, unless otherwise noted. ^1H and ^{13}C NMR spectra were measured on a Bruker Avance III 400 and 500 MHz NMR spectrometer using CDCl_3 as the solvent and using tetramethylsilane as an internal standard at room temperature. Mass analyses were recorded by auto flex MALDI-TOF mass spectrometer. Flash EA 1112 spectrometer was used to perform the elemental analyses. A suitable crystal was selected and three-dimensional X-ray data were collected on a Bruker D8 Venture diffractometer. The diffraction experiments were carried out at 100 K during data collection. Thermogravimetric analysis (TG-DTA) was performed by Bruker TG-DTA 2400SA with a heating rate of $10\text{ }^\circ\text{C min}^{-1}$ from $40\text{ }^\circ\text{C}$ to $600\text{ }^\circ\text{C}$ under nitrogen atmosphere. Fourier transform infrared (FT-IR) spectra were recorded in a wavenumber range of $400\text{-}4000\text{ cm}^{-1}$ with a Nicolet iS 10 spectrometer using the KBr pellet method.

Computational method

The calculations were performed with Gaussian 09 program using density functional theory (DFT) and time-dependent density functional theory (TD-DFT) method with B3LYP hybrid functional. All structures were optimized using DFT (S_0 state) or TD-DFT (S_1 and T_1 states) method using 6-31G(d) basis set. The contribution of atoms to frontier molecular orbitals (FMOs) and molecular planarity parameter (MPP) analysis were performed by Multiwfn software (version 3.8). Natural transition orbitals (NTOs) and energy levels of singlet and triplet excited states at their optimized S_0 geometries were conducted by time-dependent DFT calculation at B3LYP/6-31G(d) level and analysed by Multiwfn. The SOC matrix elements were calculated by TD-DFT at the B3LYP/def-TZVP level using ORCA software package (version 4.1). All calculations were performed in the gas phase.

Photophysical measurements

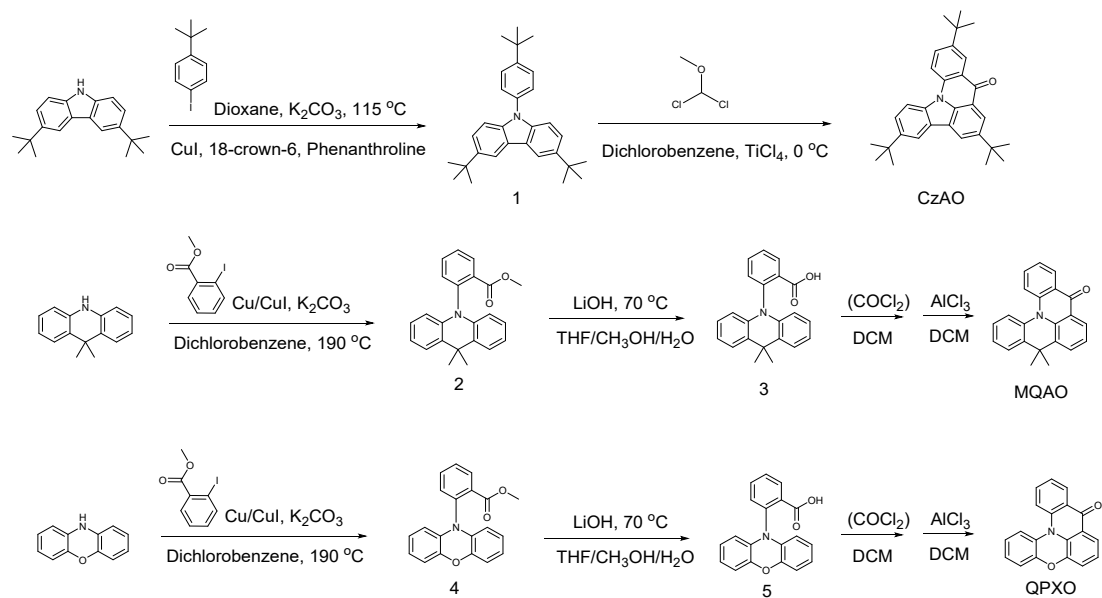
Shimadzu UV-3600I Plus spectrophotometer were applied to record UV-Vis absorption. The photoluminescence spectra were recorded on PerkinElmer LS45, while time-resolved measurements were carried out using time-correlated single-photon counting (TCSPC) spectrometer. Phosphorescence at 77 K was measured by ICCD camera with a delayed time on Edinburgh Instruments (FLS920). Quantum yields were recorded with an integrating sphere coupled with Edinburgh FS920 under ambient condition.

Ultraviolet Photoelectron Spectroscopy

The UPS measurements were performed by PHI 5000 VersaProbe III with a base pressure of the analyzer chamber in the lower 10^{-8} Pa range. The UPS spectra were recorded using He-I radiation (photon energy $E_{\text{He-I}} = 21.22\text{ eV}$) generated in a

differentially pumped, windowless discharge lamp. The measurements were performed with an applied bias of -5 V. To prepare the samples for UPS measurements, a 1 mg/ml solution of the small molecule in chlorobenzene was stirred at 50 °C for at least 1 h, in a nitrogen-filled glove box. ITO substrates were cleaned with isopropyl alcohol, acetone, detergent and deionized water in an ultrasonic bath, followed by a 15 min UV-ozone treatment, and cut the ITO substrate into 0.5 cm x 1 cm. The solution was subsequently spin coated at 1000 rpm for 60 s inside the glove box on cleaned ITO substrates. Samples were transferred through air to the UPS setup.

Synthesis



Scheme S1. Synthetic routes of CzAO, MQAO and QP XO

Synthesis of 3,6-di-*tert*-butyl-9-(4-(*tert*-butyl)phenyl)-9H-carbazole (Compound 1):

A mixture of 3,6-di-*tert*-butyl-9H-carbazole (13.43 g, 48 mmol), 1-(*tert*-butyl)-4-iodobenzene (15.00 g, 58 mmol), cuprous iodide (910 mg, 4.8 mmol), o-phenanthroline (1.73 g, 9.6 mmol), 18-crown-6 (1.90 g, 7.2 mmol) and potassium carbonate (19.87 g, 14.4 mmol) were dissolved in dry dioxane (100 mL) after the reaction system was evacuated under vacuum and purged with dry nitrogen for three times. The mixture was under stirring and heated under reflux overnight. After cooled to room temperature, the mixture was concentrated under reduced pressure to remove dioxane. Organic layer was extracted with dichloromethane / water for three times, then dried over anhydrous MgSO₄. The crude product was chromatographed on silica gel (PE / DCM = 5:1) to afford 3,6-di-*tert*-butyl-9-(4-(*tert*-butyl)phenyl)-9H-

carbazole (17.91 g, 90.68%) as a white powder. ^1H NMR (500 MHz, CDCl_3) δ 8.14 (d, J = 1.7 Hz, 2H), 7.57 (d, J = 8.5 Hz, 2H), 7.48 – 7.42 (m, 4H), 7.35 (d, J = 8.6 Hz, 2H), 1.46 (s, 18H), 1.41 (s, 9H). ^{13}C NMR (101 MHz, CDCl_3) δ 149.91, 142.61, 139.39, 135.47, 126.63, 126.25, 126.22, 123.52, 123.26, 116.21, 109.38, 34.79, 32.13, 31.53, 31.50. MALDI-TOF MS (mass m/z): 411.29243 [M] $^+$; calcd for $\text{C}_{30}\text{H}_{37}\text{N}$: 411.29260. Elemental Analysis: C, 87.54; H, 9.06; N, 3.40; found: C, 80.50; H, 9.11; N, 3.35.

Synthesis of 3,6,10-tri-*tert*-butyl-8H-indolo[3,2,1-de]acridin-8-one (CzAO):

Compound **1** (4.93g, 12 mmol) and dichloromethyl methyl ether (1.93 g, 16.8 mmol) were dissolved in 20 mL 1,2-dichlorobenzene. After the solution was cooled to 0 °C, TiCl_4 (3.64 g, 19.2mmol) was added under the nitrogen atmosphere. The mixture was stirred at room temperature for 4 hours. The reaction mixture was quenched by adding hydrochloric acid and extracted with dichloromethane / water for three times, then dried over anhydrous MgSO_4 . The crude product was chromatographed on silica gel (PE/DCM = 2:1) to afford 3,6,10-tri-*tert*-butyl-8H-indolo[3,2,1-de]acridin-8-one as a light yellow powder (1.84 g, 35%). ^1H NMR (400 MHz, CDCl_3) δ 8.69 (d, J = 2.3 Hz, 1H), 8.51 (d, J = 1.2 Hz, 1H), 8.45 (d, J = 1.5 Hz, 1H), 8.36 (d, J = 8.9 Hz, 1H), 8.24 – 8.15 (m, 2H), 7.92 (dd, J = 8.8, 2.3 Hz, 1H), 7.66 (dd, J = 8.7, 1.7 Hz, 1H), 1.55 (s, 9H), 1.50 (s, 9H), 1.47 (s, 9H). ^{13}C NMR (101 MHz, CDCl_3) δ 179.11, 146.48, 146.10, 146.01, 137.65, 137.52, 137.29, 131.60, 126.52, 125.24, 125.13, 125.01, 124.74, 122.55, 121.02, 119.08, 117.97, 115.26, 113.38, 35.46, 34.88, 34.79, 32.05, 31.79, 31.43. MALDI-TOF MS (mass m/z): 437.27146 [M] $^+$; calcd for $\text{C}_{31}\text{H}_{35}\text{NO}$: 437.27186. Elemental Analysis: C, 85.08; H, 8.06; N, 3.20; O, 3.66; found: C, 85.10; H, 8.04; N, 3.22 , O, 3.64. IR (KBr): 2961, 1654, 1613, 1493, 1267, 804 cm^{-1} .

Synthesis of methyl 2-(9,9-dimethylacridin-10(9H)-yl)benzoate (Compound 2):

9,9-dimethyl-9,10-dihydroacridine (4.18 g, 20 mmol), methyl 2-iodobenzoate (5.76 g, 22 mmol), potassium carbonate (3.03 g, 22 mmol), activated copper powder (1.3 mg, 20 mmol) and cuprous iodide(381 mg, 2 mmol) were dissolved in 30 mL 1,2-dichlorobenzene after the reaction system was evacuated under vacuum and purged with dry nitrogen for three times. The reaction mixture was heated to 190°C for 48 h. After cooled to room temperature, the reaction was filtered, the solvent removed

under vacuum condition, and then the residue purified by column chromatography on silica gel (PE/DCM = 2:1) to afford methyl 2-(9,9-dimethylacridin-10(9H)-yl)benzoate as a light green powder (5.89 g, 85.8%). ¹H NMR (400 MHz, CDCl₃) δ 8.20 – 8.14 (m, 1H), 7.76 (td, *J* = 7.7, 1.5 Hz, 1H), 7.63 – 7.56 (m, 1H), 7.45 (dd, *J* = 7.5, 1.5 Hz, 2H), 7.34 (d, *J* = 7.8 Hz, 1H), 6.97 – 6.85 (m, 4H), 6.05 (d, *J* = 9.1 Hz, 2H), 3.54 (s, 3H), 1.71 (d, *J* = 22.8 Hz, 6H). ¹³C NMR (126 MHz, CDCl₃) δ 165.95, 140.70, 140.43, 134.58, 133.41, 132.74, 132.35, 129.59, 128.56, 126.37, 125.64, 120.35, 113.53, 52.34, 35.87, 33.24, 31.81. MALDI-TOF MS (mass m/z): 343.15698 [M]⁺; calcd for C₂₃H₂₁NO₂: 343.15723. Elemental Analysis: C, 80.44; H, 6.16; N, 4.08; O, 9.32; found: C, 80.43; H, 6.18; N, 4.09, O, 9.33.

Synthesis of 2-(9,9-dimethylacridin-10(9H)-yl)benzoic acid (Compound 3):

Compound 2 (5.83 g, 17 mmol) and lithium hydroxide (1.22 g, 51 mmol) in a solution of 3:1:1 tetrahydrofuran/methanol/water (40 mL) heated to 70 °C for 12 h. Acidification with concentrated hydrochloric acid precipitated the light yellow powder 2-(9,9-dimethylacridin-10(9H)-yl)benzoic acid, which was collected by vacuum filtration and oven-dried (80 °C) overnight, then employed directly without further purification. Yield: 5.5 g (98.3%). ¹H NMR (400 MHz, CDCl₃) δ 8.20 – 8.14 (m, 1H), 7.76 (td, *J* = 7.7, 1.5 Hz, 1H), 7.63 – 7.56 (m, 1H), 7.45 (dd, *J* = 7.5, 1.5 Hz, 2H), 7.34 (d, *J* = 7.8 Hz, 1H), 6.97 – 6.85 (m, 4H), 6.05 (d, *J* = 9.1 Hz, 2H), 3.54 (s, 3H), 1.71 (d, *J* = 22.8 Hz, 6H). ¹³C NMR (126 MHz, CDCl₃) δ 165.95, 140.70, 140.43, 134.58, 133.41, 132.74, 132.35, 129.59, 128.56, 126.37, 125.64, 120.35, 113.53, 52.34, 35.87, 33.24, 31.81. MALDI-TOF MS (mass m/z): 329.14129 [M]⁺; calcd for C₂₂H₁₉NO₂: 329.14158. Elemental Analysis: C, 80.22; H, 5.81; N, 4.25; O, 9.71; found: C, 80.23; H, 5.81; N, 4.24, O, 9.72.

Synthesis of 9,9-dimethylquinolino[3,2,1-de]acridin-5(9H)-one (MQAO):

Compound 3 (4.9 g, 15 mmol) was dispersed in dry dichloromethane (30 mL). Two drops of N,N-dimethylformamide was added followed by oxalyl chloride (9.52 g, 75 mol) at 0 °C and then the reaction was stirred to at room temperature for 4 hours until all of it was dissolved. The mixture was concentrated under reduced pressure to remove solvent. After adding 30 mL dichloromethane, added aluminum trichloride (8 g, 60 mmol) to the system and reacted at room temperature for 30 min. The reaction mixture was added dropwise to 50 mL hydrochloric acid (1M) and extracted with

dichloromethane. The organic layer dried over sodium sulfate and concentrated. The crude product was then by column chromatography on silica gel (PE/DCM = 1:1) to afford **MQAO** as a yellow powder (3.1 g, 66.4%). This compound was further purified by sublimation before used in device fabrication. ¹H NMR (400 MHz, CDCl₃) δ 8.53 – 8.48 (m, 1H), 8.34 – 8.28 (m, 1H), 8.04 (d, *J* = 8.5 Hz, 1H), 7.78 – 7.73 (m, 1H), 7.69 – 7.57 (m, 3H), 7.39 (td, *J* = 7.8, 2.8 Hz, 2H), 7.23 (dd, *J* = 7.5, 5.6 Hz, 2H), 2.01 (s, 3H), 1.36 (s, 3H). ¹³C NMR (101 MHz, CDCl₃) δ 179.30, 140.16, 139.16, 137.43, 137.24, 135.27, 132.31, 127.59, 127.46, 126.29, 125.41, 125.32, 124.44, 124.42, 123.39, 123.27, 123.13, 119.82, 119.44, 37.03, 31.08, 23.05. MALDI-TOF MS (mass m/z): 311.13088 [M]⁺; calcd for C₂₂H₁₇NO: 311.13101. Elemental Analysis: C, 84.86; H, 5.50; N, 4.50; O, 5.14; found: C, 84.87; H, 5.52; N, 4.51, O, 5.12. IR (KBr): 2970, 1642, 1601, 1474, 1429, 1288, 775 cm⁻¹.

Synthesis of methyl 2-(10H-phenoxazin-10-yl)benzoate (Compound 4):

A method similar to the synthesis of Compound 2 was implemented except that 10H-phenoxazine (5.49 g, 30 mmol) was used instead of 9,9-dimethyl-9,10-dihydroacridine, resulting in a yellow solid (7.29 g, 76.5%). ¹H NMR (400 MHz, CDCl₃) δ 8.18 – 8.10 (m, 1H), 7.78 – 7.71 (m, 1H), 7.56 (t, *J* = 7.6 Hz, 1H), 7.40 (d, *J* = 7.7 Hz, 1H), 6.69 – 6.52 (m, 6H), 5.78 (d, *J* = 9.0 Hz, 2H), 3.71 (s, 3H). ¹³C NMR (126 MHz, CDCl₃) δ 165.78, 143.86, 138.53, 134.69, 134.07, 133.33, 133.12, 131.65, 128.87, 123.18, 121.26, 115.41, 112.90, 52.55. ¹³C NMR (126 MHz, CDCl₃) δ 167.67, 144.08, 140.08, 135.79, 133.65, 132.84, 130.37, 129.07, 123.32, 122.02, 115.64, 113.87. MALDI-TOF MS (mass m/z): 317.10502 [M]⁺; calcd for C₂₀H₁₅NO₃: 317.10519. Elemental Analysis: C, 75.70; H, 4.76; N, 4.41; O, 15.12; found: C, 75.71; H, 4.77; N, 4.42, O, 15.12.

Synthesis of 2-(10H-phenoxazin-10-yl)benzoic acid (Compound 5):

Using a similar synthetic procedure for Compound 3 by hydrolysis reaction, yellow solid was finally obtained, and then used directly for next step without further purification. Yield: 6 g (99%). ¹H NMR (400 MHz, CDCl₃) δ 8.29 (d, *J* = 7.8 Hz, 1H), 7.84 – 7.74 (m, 1H), 7.58 (t, *J* = 7.6 Hz, 1H), 7.42 (d, *J* = 7.8 Hz, 1H), 6.78 – 6.62 (m, 4H), 6.62 – 6.48 (m, 2H), 5.81 (d, *J* = 7.8 Hz, 2H). ¹³C NMR (126 MHz, CDCl₃) δ 167.67, 144.08, 140.08, 135.79, 133.65, 132.84, 130.37, 129.07, 123.32, 122.02, 115.64, 113.87. MALDI-TOF MS (mass m/z): 303.08926 [M]⁺; calcd for C₁₉H₁₃NO₃:

303.08954. Elemental Analysis: C, 75.24; H, 4.32; N, 4.62; O, 15.82; found: C, 75.23; H, 4.31; N, 4.61, O, 15.82.

Synthesis of 9H-quinolino[3,2,1-kl]phenoxazin-9-one (QPXO):

Using a similar synthetic procedure for **MQAO**, yellow solid was finally obtained. Yield: 640 mg (45%). ¹H NMR (400 MHz, CDCl₃) δ 8.52 – 8.46 (m, 1H), 8.05 (d, *J* = 8.6 Hz, 1H), 7.97 (dd, *J* = 6.6, 2.8 Hz, 1H), 7.67 (ddd, *J* = 8.6, 7.2, 1.5 Hz, 1H), 7.58 (d, *J* = 8.1 Hz, 1H), 7.37 (t, *J* = 7.5 Hz, 1H), 7.24 – 7.17 (m, 2H), 7.14 (d, *J* = 4.0 Hz, 2H), 7.07 (dt, *J* = 8.8, 4.4 Hz, 1H). ¹³C NMR (101 MHz, CDCl₃) δ 177.62, 148.25, 146.28, 138.35, 133.16, 132.62, 128.35, 127.88, 126.10, 124.81, 123.78, 123.74, 123.40, 123.29, 120.62, 118.26, 118.19, 118.06, 117.62. MALDI-TOF MS (mass m/z): 285.07871 [M]⁺; calcd for C₁₉H₁₁NO₂: 285.07898. Elemental Analysis: C, 79.99; H, 3.89; N, 4.91; O, 11.22; found: C, 79.98; H, 3.88; N, 4.91, O, 11.23. IR (KBr): 1650, 1620, 1602, 1484, 1293, 747 cm⁻¹.

Synthesis of QPO

QPO was obtained as a yellow solid according to the literature.¹

Table S1. Crystal data and structure refinement for **CzAO**, **MQAO**, **QPXO** and **QPO**.

Identification code	CzAO	MQAO	QPXO	QPO
Empirical formula	C ₃₁ H ₃₅ NO	C ₂₂ H ₁₇ NO	C ₁₉ H ₁₁ NO ₂	C ₁₉ H ₁₁ NOS
Formula weight	437.60	311.36	285.29	301.35
Temperature/K	170.0	170.0	170	100.0
Crystal system	monoclinic	triclinic	orthorhombic	orthorhombic
Space group	P2 ₁ /n	P-1	Pbca	Pbca
a/Å	12.0537(10)	8.6697(7)	16.5609(16)	16.3178(4)
b/Å	13.4766(11)	9.9227(8)	7.5103(9)	8.1324(2)
c/Å	30.162(3)	10.4685(8)	20.848(2)	20.2196(6)
α/°	90	70.490(3)	90	90
β/°	93.446(3)	67.026(3)	90	90
γ/°	90	75.263(3)	90	90
Volume/Å ³	4890.8(7)	773.51(11)	2593.0(5)	2683.20(12)
Z	8	2	8	8
ρ _{calc} g/cm ³	1.189	1.337	1.462	1.492
μ/mm ⁻¹	0.070	0.082	0.096	0.241
F(000)	1888.0	328.0	1184.0	1248.0
Crystal size/mm ³	0.12 × 0.08 × 0.05	0.12 × 0.08 × 0.03	0.15 × 0.08 × 0.04	0.19 × 0.12 × 0.08
Radiation	MoKα (λ = 0.71073)	MoKα (λ = 0.71073)	MoKα (λ = 0.71073)	MoKα (λ = 0.71073)
2Θ range for data collection/°	4.056 to 52.84	4.382 to 52.866	4.92 to 52.9	4.74 to 52.758
Index ranges	-15 ≤ h ≤ 15, -16 ≤ k ≤ 16, -37 ≤ l ≤ 37	-10 ≤ h ≤ 10, -12 ≤ k ≤ 11, -13 ≤ l ≤ 12	-20 ≤ h ≤ 0, -9 ≤ k ≤ 9, 0 ≤ l ≤ 26	-19 ≤ h ≤ 20, -10 ≤ k ≤ 10, -25 ≤ l ≤ 25
Reflections collected	40415	8675	4904	23433
Independent reflections	9922 [Rint = 0.1053, Rsigma = 0.1044]	3145 [Rint = 0.0345, Rsigma = 0.0427]	2658 [Rint = 0.0482, Rsigma = 0.0637]	2733 [Rint = 0.0645, Rsigma = 0.0325]
Data/restraints/parameters	9922/0/613	3145/0/219	2658/6/203	2733/0/199
Goodness-of-fit on F ²	1.027	1.019	1.070	1.009
Final R indexes [I>=2σ (I)]	R ₁ = 0.0897, wR ₂ = 0.1991	R1 = 0.0475, wR2 = 0.1110	R1 = 0.0615, wR2 = 0.1298	R1 = 0.0486, wR2 = 0.1233
Final R indexes [all data]	R ₁ = 0.1862, wR ₂ = 0.2438	R1 = 0.0706, wR2 = 0.1281	R1 = 0.1082, wR2 = 0.1536	R1 = 0.0650, wR2 = 0.1369
Largest diff. peak/hole / e Å ⁻³	0.32/-0.31	0.22/-0.22	0.22/-0.25	0.55/-0.51
CCDC	2119761	2119762	2119763	2119764

Photophysical experiments

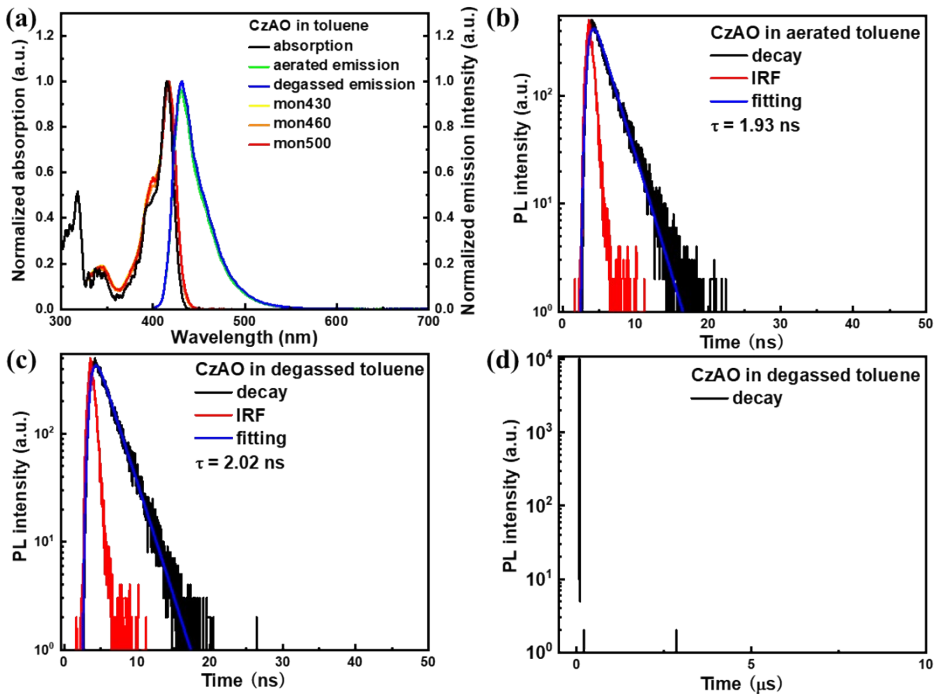


Figure S1. (a) Normalized ultraviolet-visible absorption and photoluminescence spectra ($\lambda_{\text{ex}} = 380$ nm, a.u.: arbitrary units, mon: the excitation spectrum monitored at different specified emission wavelength); Transient PL decay spectra ($\lambda_{\text{ex}} = 380$ nm) of **CzAO** in aerated (b) and (c) degassed toluene solution (1×10^{-5} M) recorded and in range of 50 ns (d) 10 μ s recorded at 298 K.

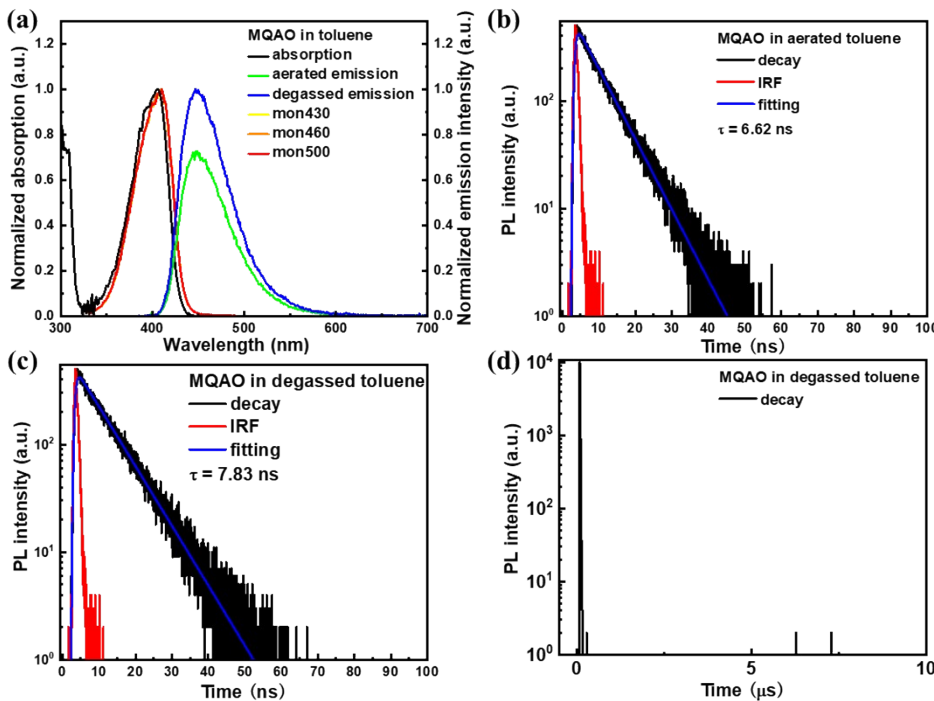


Figure S2. (a) Normalized ultraviolet-visible absorption and photoluminescence spectra ($\lambda_{\text{ex}} = 380$ nm, a.u.: arbitrary units, mon: the excitation spectrum monitored at different specified emission wavelength); Transient PL decay spectra ($\lambda_{\text{ex}} = 380$ nm) of **DQAO** in aerated (b) and (c) degassed toluene solution (1×10^{-5} M) recorded and in range of 50 ns (d) 10 μ s recorded at 298 K.

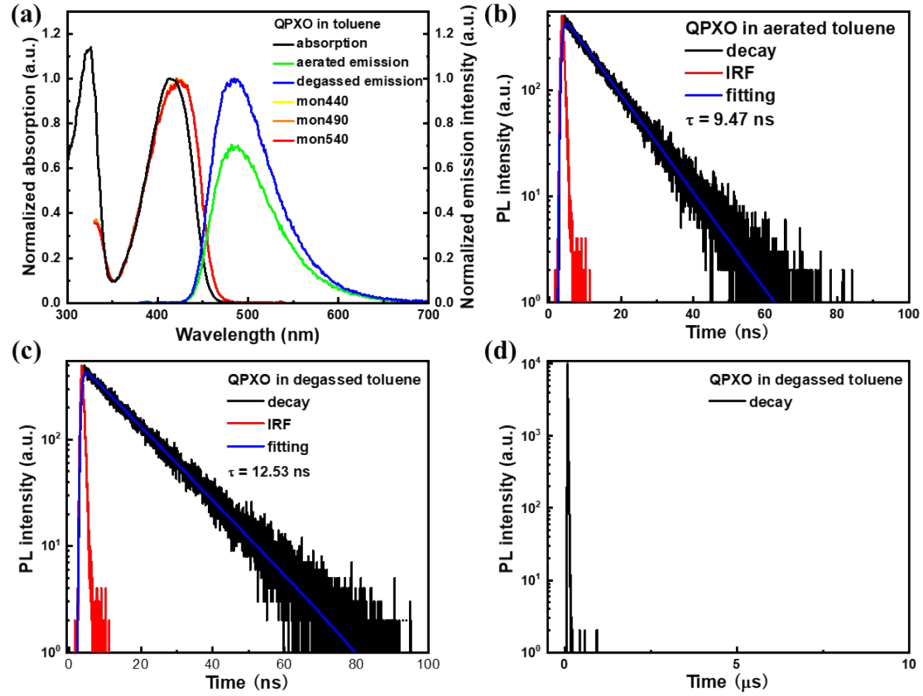


Figure S3. (a) Normalized ultraviolet-visible absorption and photoluminescence spectra ($\lambda_{\text{ex}} = 380$ nm, a.u.: arbitrary units, mon: the excitation spectrum monitored at different specified emission wavelength); Transient PL decay spectra ($\lambda_{\text{ex}} = 380$ nm) of **QP XO** in aerated (b) and (c) degassed toluene solution (1×10^{-5} M) recorded and in range of 50 ns (d) 10 μ s recorded at 298 K.

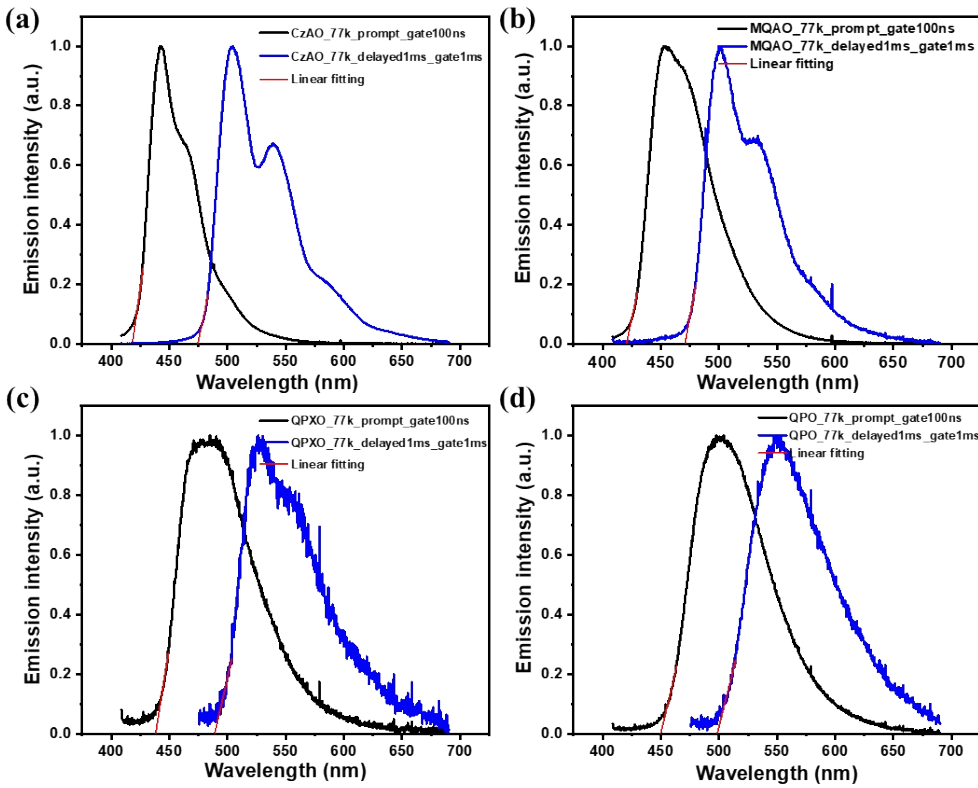


Figure S4. Normalized fluorescence (delay=0 ns, gate width 100 ns; $\lambda_{\text{ex}} = 380 \text{ nm}$) and phosphorescence spectra (delay 1 ms, gate width 1 ms; $\lambda_{\text{ex}} = 380 \text{ nm}$) of (%) (a) CzAO, (b) MQAO, (c) QP XO and (d) QPO in degassed toluene solution ($1 \times 10^{-5} \text{ M}$, 77 K).

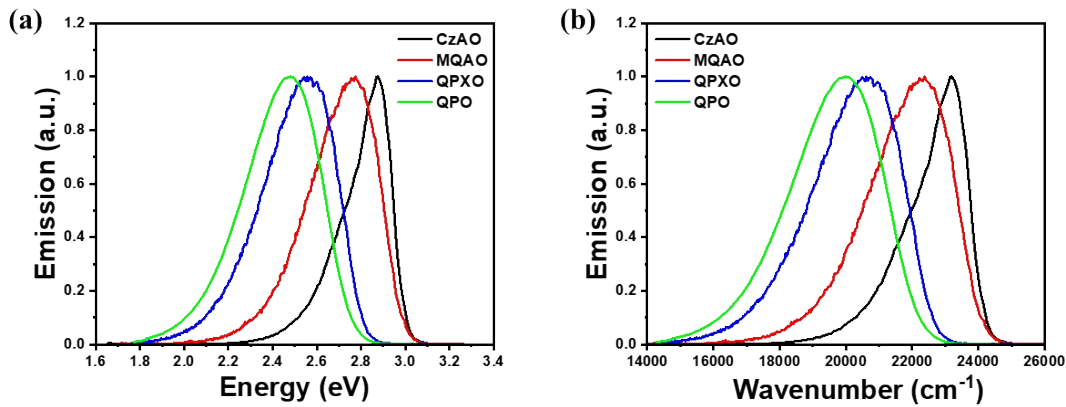


Figure S5. Photoluminescence spectra in terms of Energy (a) and Wavenumber(b) of the investigated molecules

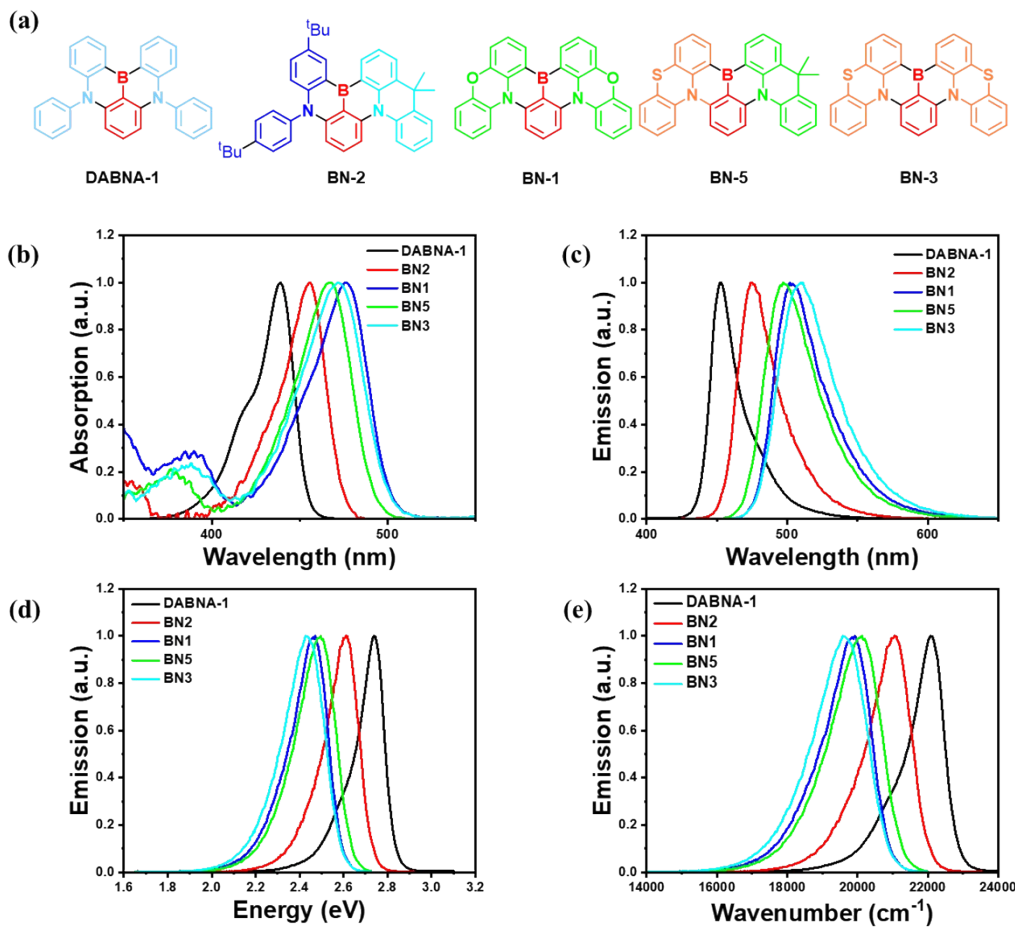


Figure S6. (a) Chemical structures, (b) UV–vis absorption spectra, Photoluminescence spectra in terms of wavelength (c), Energy (d) and Wavenumber(e) of the investigated molecules

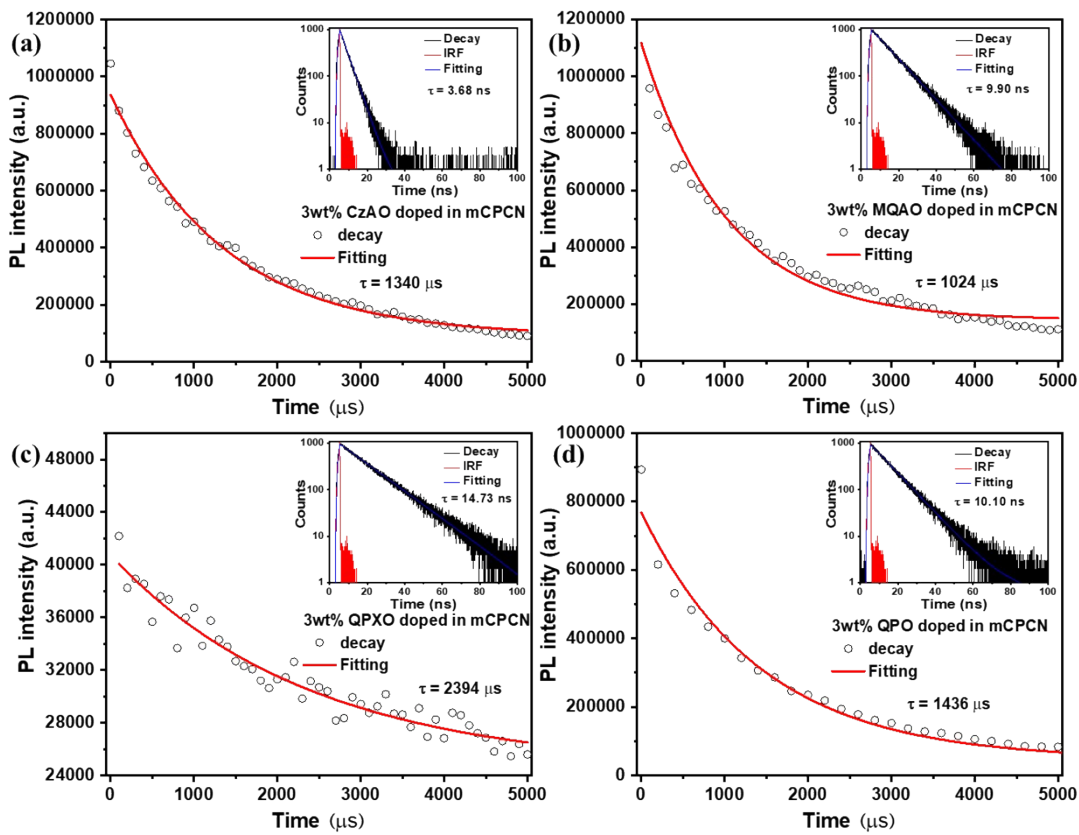


Figure S7. Transient decay profile of the mCPCN:(3wt%) (a) CzAO, (b) MQAO, (c) QP XO and (d) QPO film at 298 K in range of 5000 ms detected by intensified charge-coupled device (ICCD) per 20 ms with 10 ms gate width shows a delayed fluorescence component fitted with a single exponential decay.

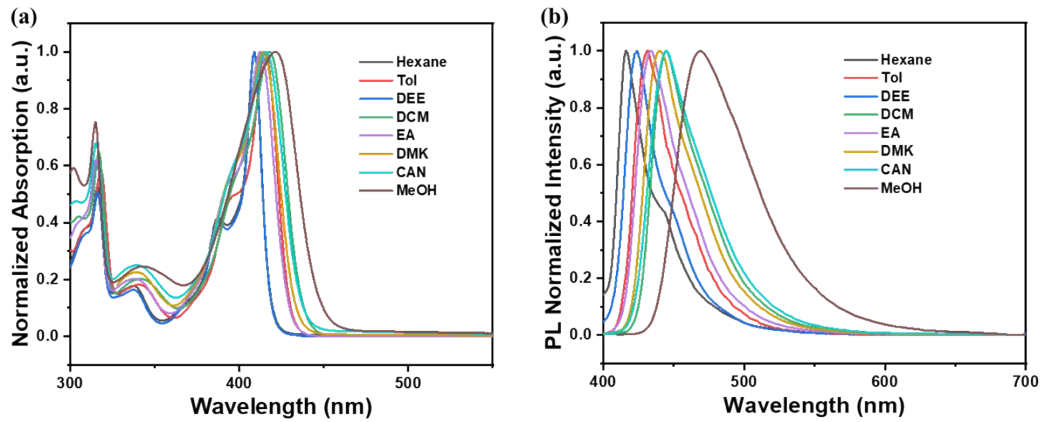


Figure S8. (a) UV-vis absorption spectra and (c) Photoluminescence spectra of CzAO in various solvents.

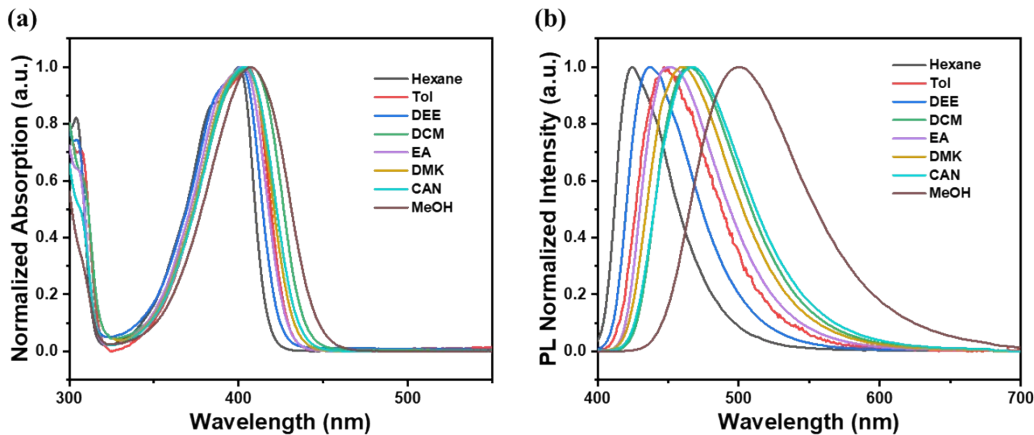


Figure S9. (a) UV–vis absorption spectra and (c) Photoluminescence spectra of MQAO in various solvents.

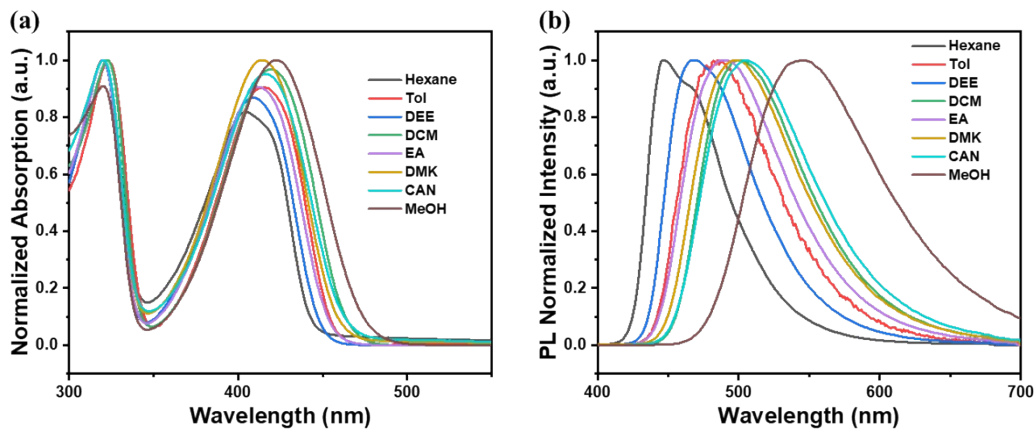


Figure S10. (a) UV–vis absorption spectra and (c) Photoluminescence spectra of QP XO in various solvents.

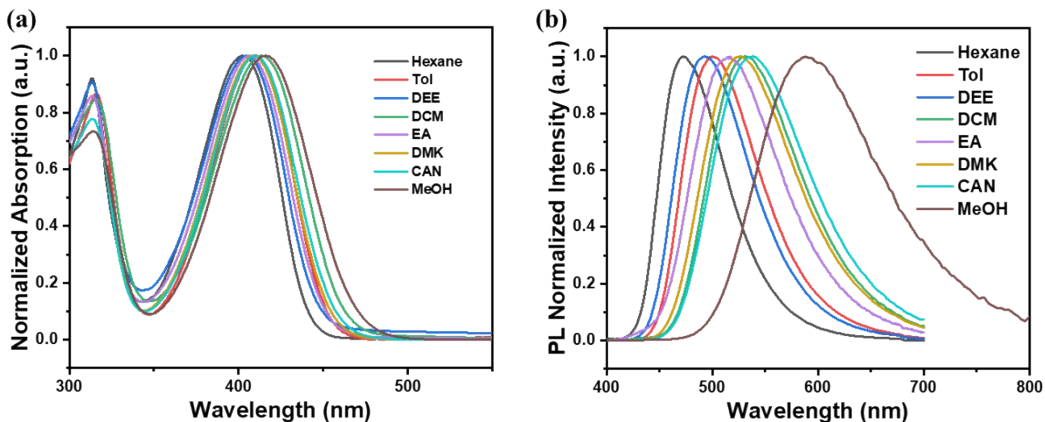


Figure S11. (a) UV–vis absorption spectra and (c) Photoluminescence spectra of QPO in various solvents.

Table S2. Comparison photophysical properties of reported B/N and Carbonyl/Amine system molecules

System	Compound	λ_{abs} (nm)	λ_{em} (nm)	FWHM (nm/eV)	Stoke shift (cm $^{-1}$)	Ref.
B/N	DABNA-1	439	453	24/0.140	704	2
	BN-2	456	475	34/0.178	877	3
	BN-1	476	502	41/0.197	1088	
	BN-5	467	497	44/0.215	1292	
	BN-3	472	511	46/0.221	1617	
Carbonyl/Amine	QAO	433	460	33	1356	4
	DQAO	440	465	33	1222	
	OQAO	489	520	36	1293	
	SQAO	489	552	54	2334	

Table S3. Summary of emission peak, FWHM with nm and eV in various solvents along with their relative polarity.

	Hexane (Hex)	Duethyl Ether (DEE)	Toluene (Tol)	Ethyl Acetate (EA)	Acetone (DMK)	Dichloromethane (DCM)	Acetonitrile (CAN)	Methanol (MeOH)
Relative polarity	0.009	0.145	0.099	0.228	0.355	0.309	0.460	0.762
CzAO	λ_{em} (nm)	416	424	431	434	440	444	444
	FWHM (nm / eV)	26/0.18	30/0.20	36/0.23	38/0.24	41/0.25	41/0.25	47/0.28
MQAO	λ_{em} (nm)	424	437	447	451	460	464	467
	FWHM (nm / eV)	45/0.30	54/0.34	61/0.36	64/0.37	69/0.39	69/0.38	73/0.40
QPXO	λ_{em} (nm)	447	467	485	488	498	501	505
	FWHM (nm / eV)	61/0.35	71/0.38	76/0.39	83/0.41	87/0.42	86/0.41	90/0.42
QPO	λ_{em} (nm)	472	493	501	515	527	531	539
	FWHM (nm / eV)	73/0.39	83/0.41	86/0.41	99/0.45	103/0.45	101/0.43	109/0.45

Theoretical simulations

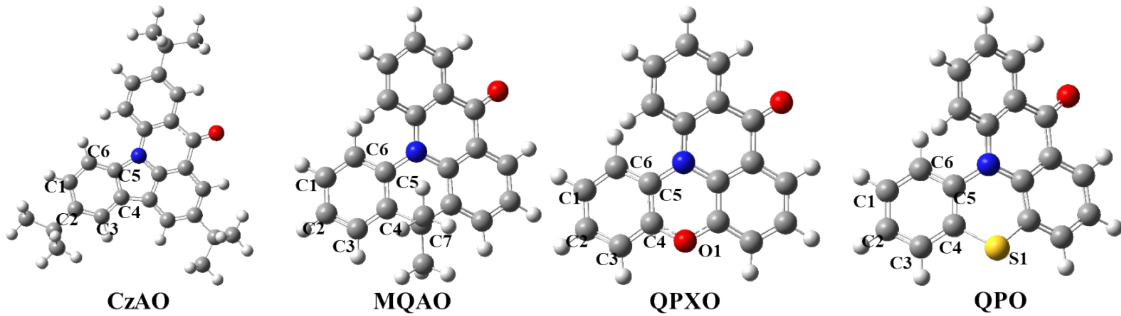


Figure S12. Atoms involved in peripheral moieties for **CzAO**, **MQAO**, **QP XO** and **QPO**.

Table S4. The selected atoms contribution to HOMO and LUMO for **CzAO**, **MQAO**, **QP XO** and **QPO** by orbital composition analysis.

Atom	Contribution(%)							
	CzAO		MQAO		QP XO		QPO	
	HOMO	LUMO	HOMO	LUMO	HOMO	LUMO	HOMO	LUMO
C1	0.118	3.117	0.438	0.641	3.024	0.041	2.24	0.334
C2	7.704	0.681	7.23	0.804	5.314	0.856	4.444	0.580
C3	3.838	1.917	0.788	0.106	0.723	0.180	0.510	0.065
C4	2.907	2.503	4.754	1.112	5.87	0.494	5.418	0.881
C5	1.243	2.577	3.570	0.650	5.101	0.381	4.772	0.433
C6	7.638	0.082	5.366	0.251	2.442	0.691	2.198	0.244
C7/O1/S1	-	-	0.379	0.020	8.914	0.748	19.397	0.953
Summury	23.448	10.877	22.525	3.584	31.388	3.391	38.979	3.490
Deviation ^a	12.571		18.941		27.997		35.489	

a: Deviation = HOMO (summury) – LUMO (summury).

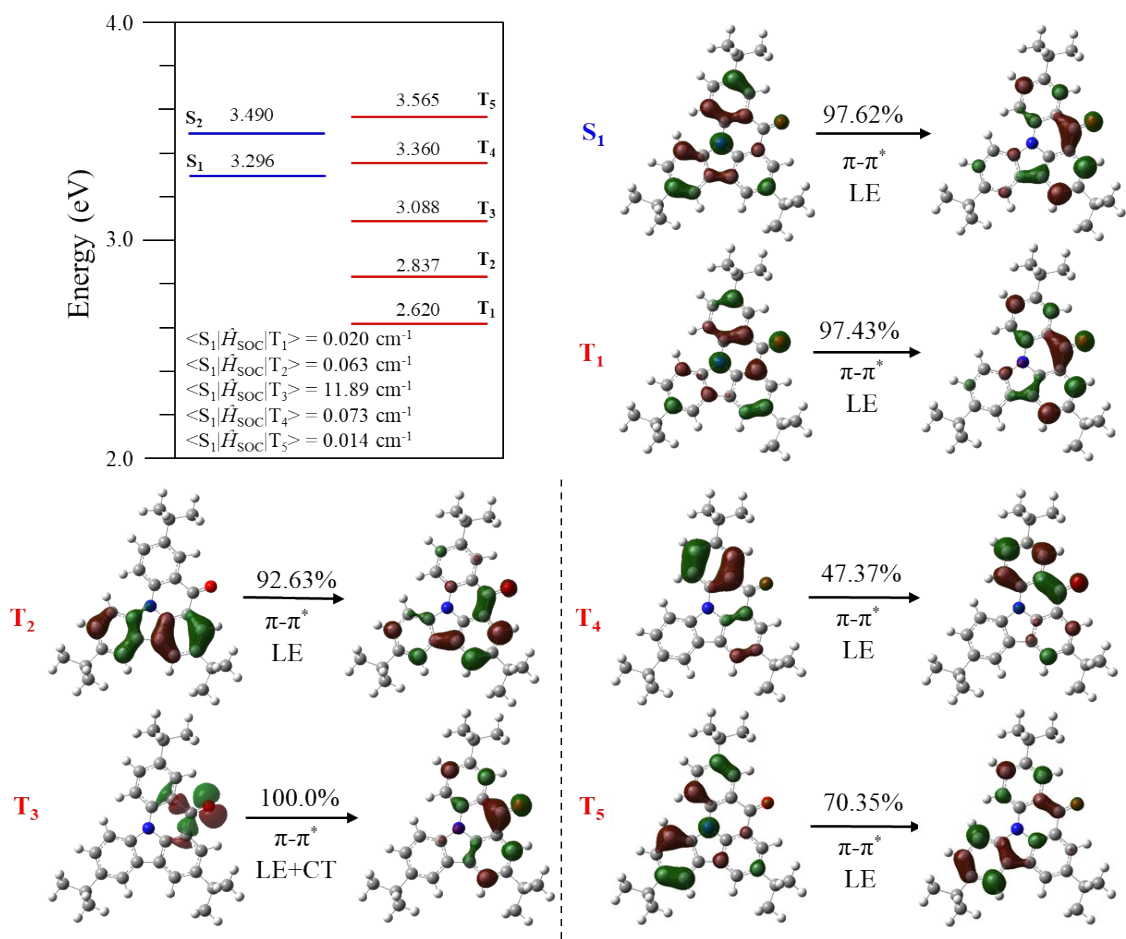


Figure S13. Energy-level diagrams and associated natural transition orbitals (NTOs) and spin-orbit coupling (SOC) matrix elements for the singlet (S_1) and triplet (T_n) excited states of CzAO.

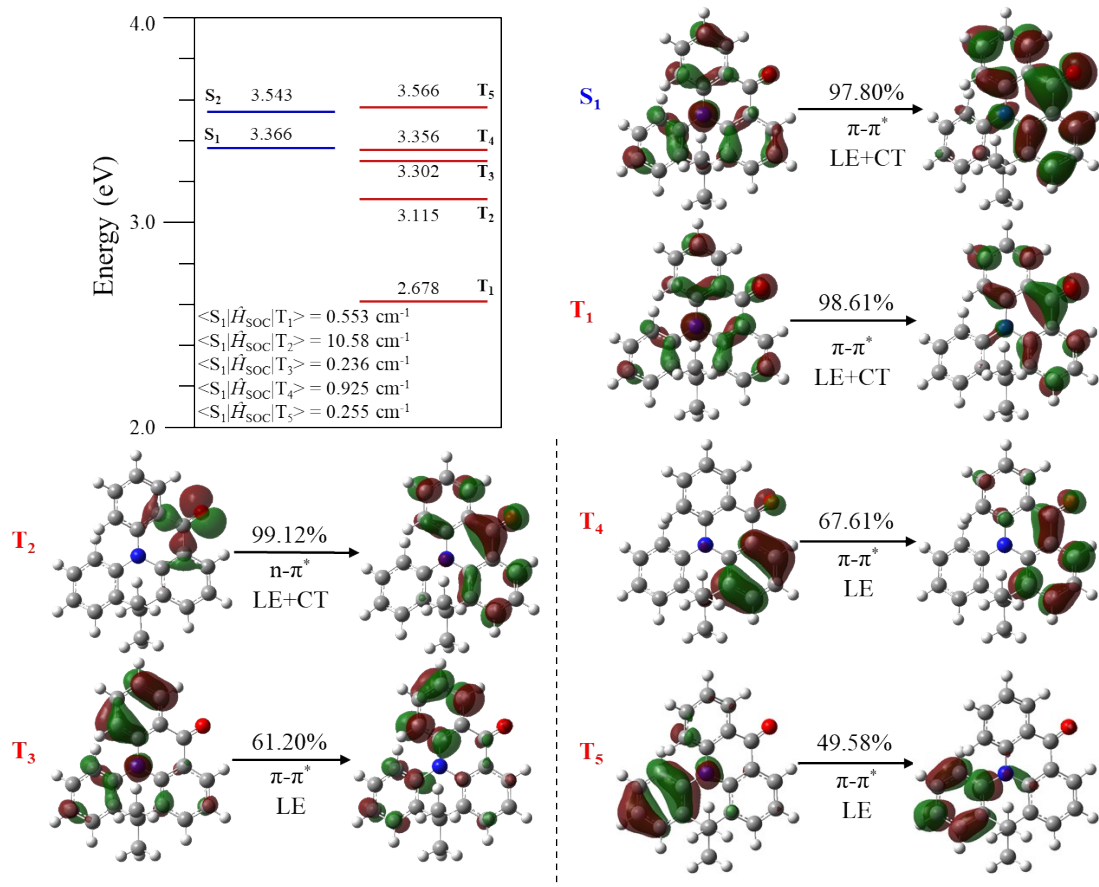


Figure S14. Energy-level diagrams and associated natural transition orbitals (NTOs) and spin-orbit coupling (SOC) matrix elements for the singlet (S_1) and triplet (T_n) excited states of MQAO.

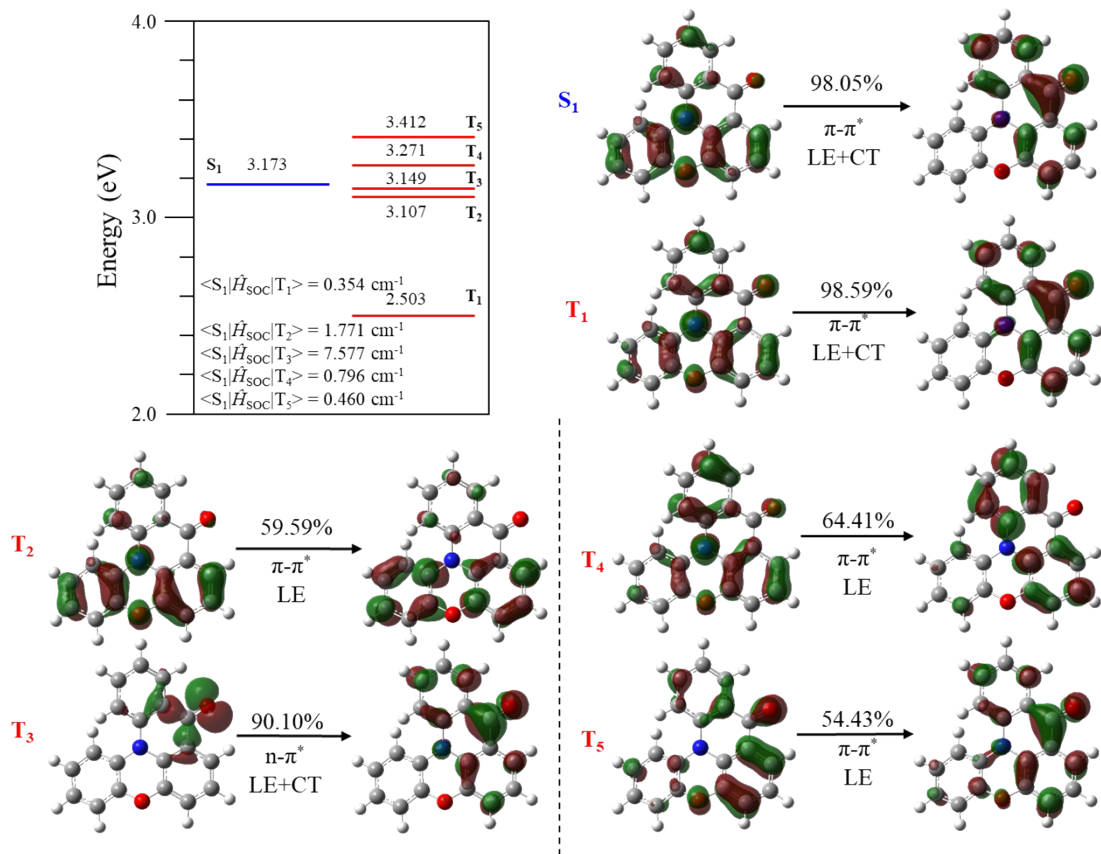


Figure S15. Energy-level diagrams and associated natural transition orbitals (NTOs) and spin-orbit coupling (SOC) matrix elements for the singlet (S_1) and triplet (T_n) excited states of QP XO.

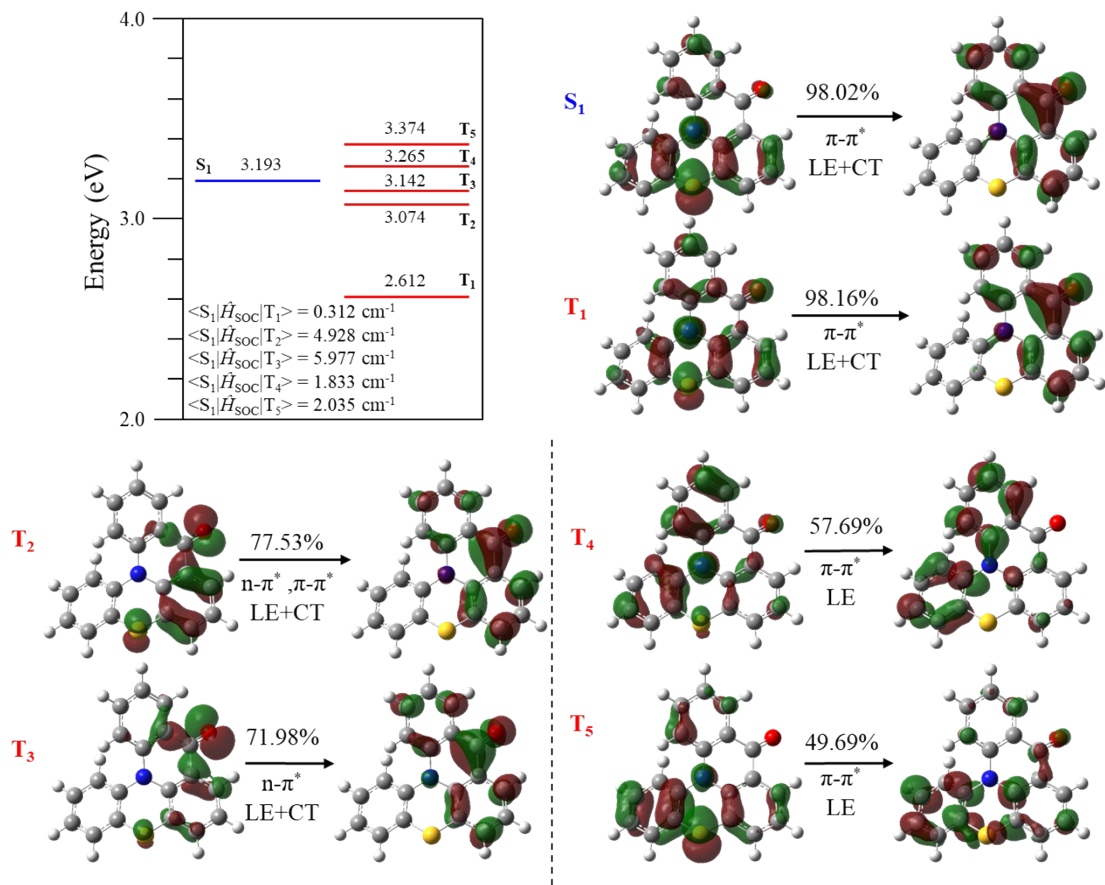


Figure S16. Energy-level diagrams and associated natural transition orbitals (NTOs) and spin-orbit coupling (SOC) matrix elements for the singlet (S_1) and triplet (T_n) excited states of QPO.

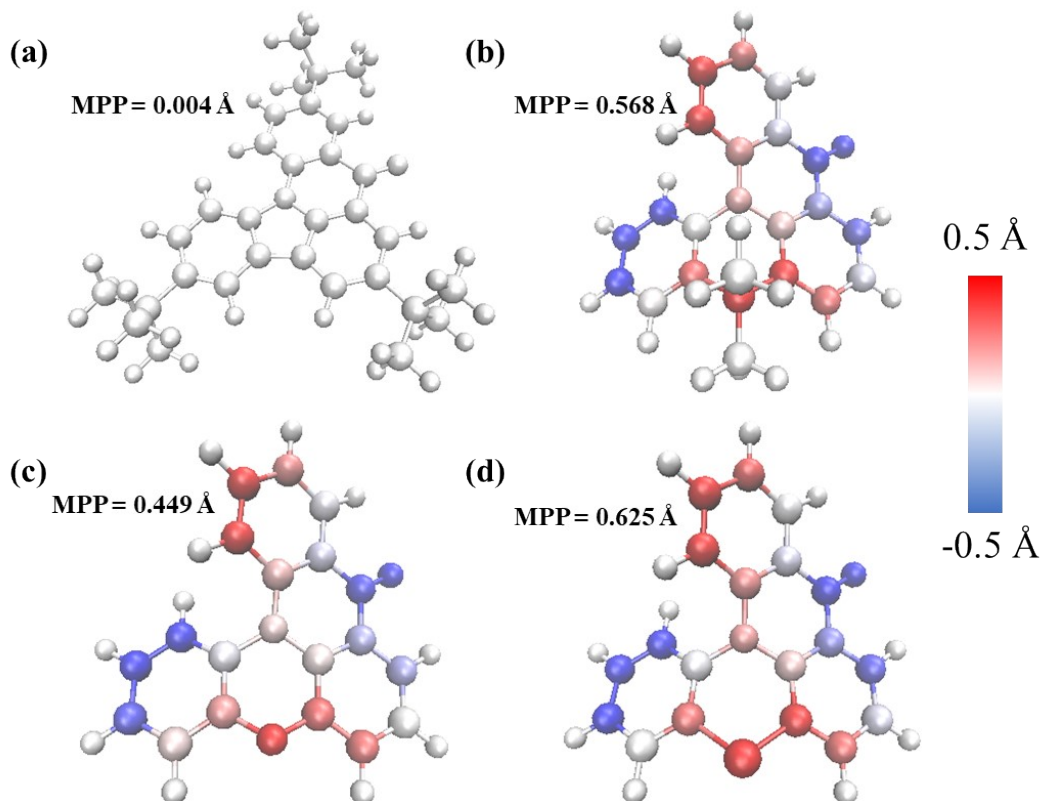


Figure S17. MPP calculated for (a) **CzAO**, (b) **MQAO**, (c) **QP XO**, (d) **QPO** optimized at B3LYP/6-31G(d) level. The bluer (redder) the color, the larger the distance of the atom below (above) the fitting plane.

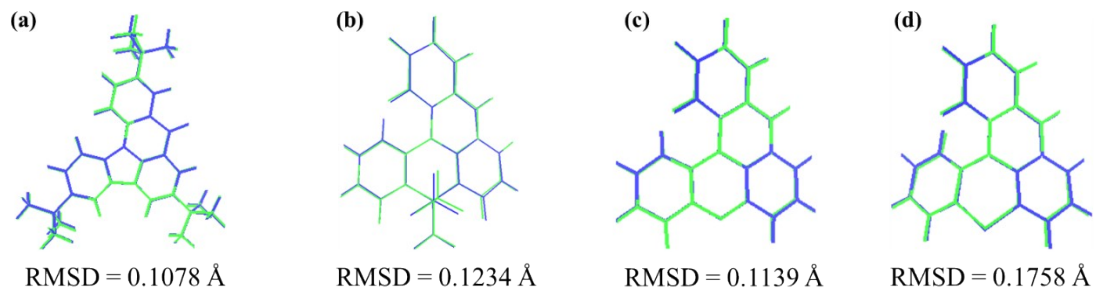


Figure S18. Comparison of the optimized structures of (a) **CzAO** (b) **MQAO** (c) **QP XO** and (d) **QPO** in the S_0 (green) and S_1 (blue) states.

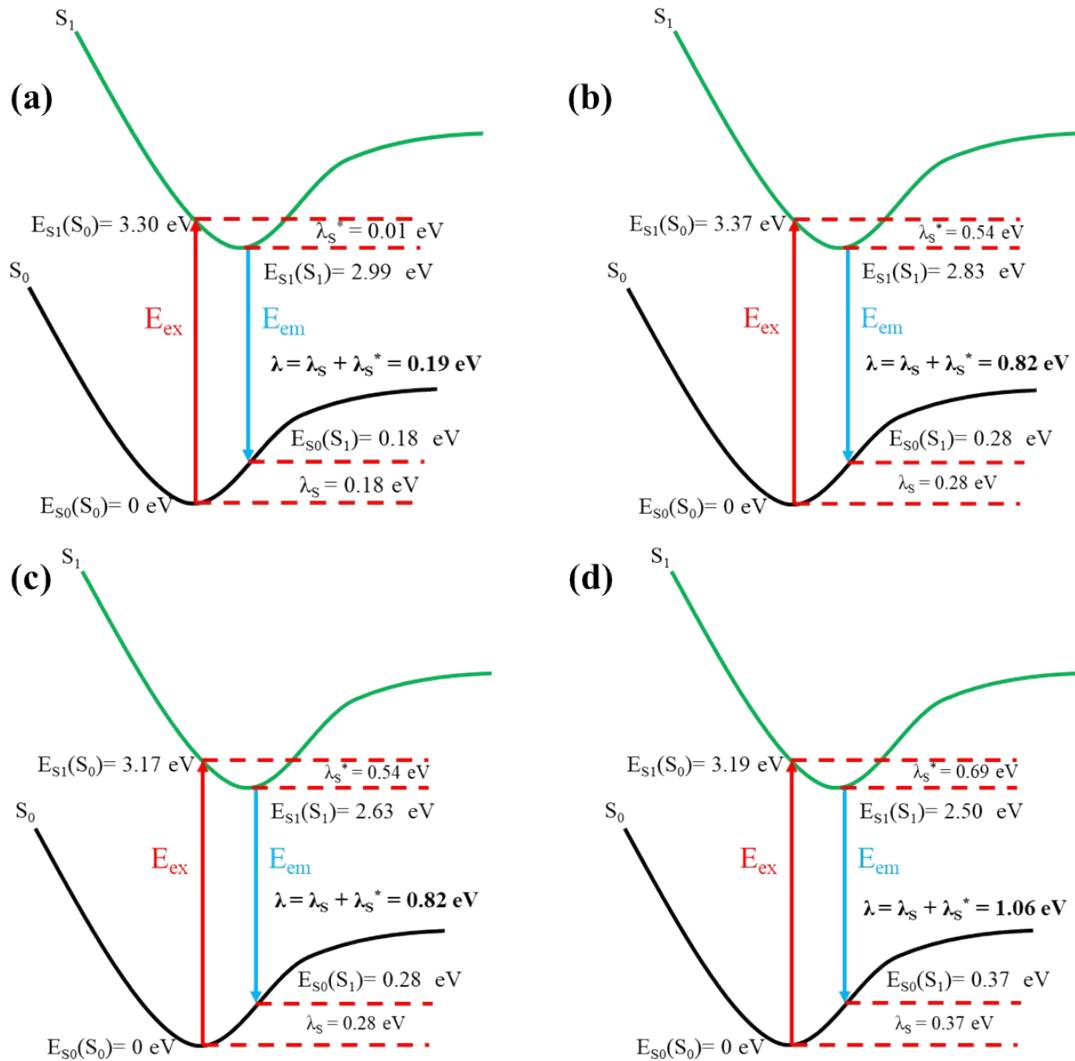


Figure S19. Single point energies, reorganization energies (λ) of (a) CzAO (b) MQAO (c) QP XO and (d) QPO

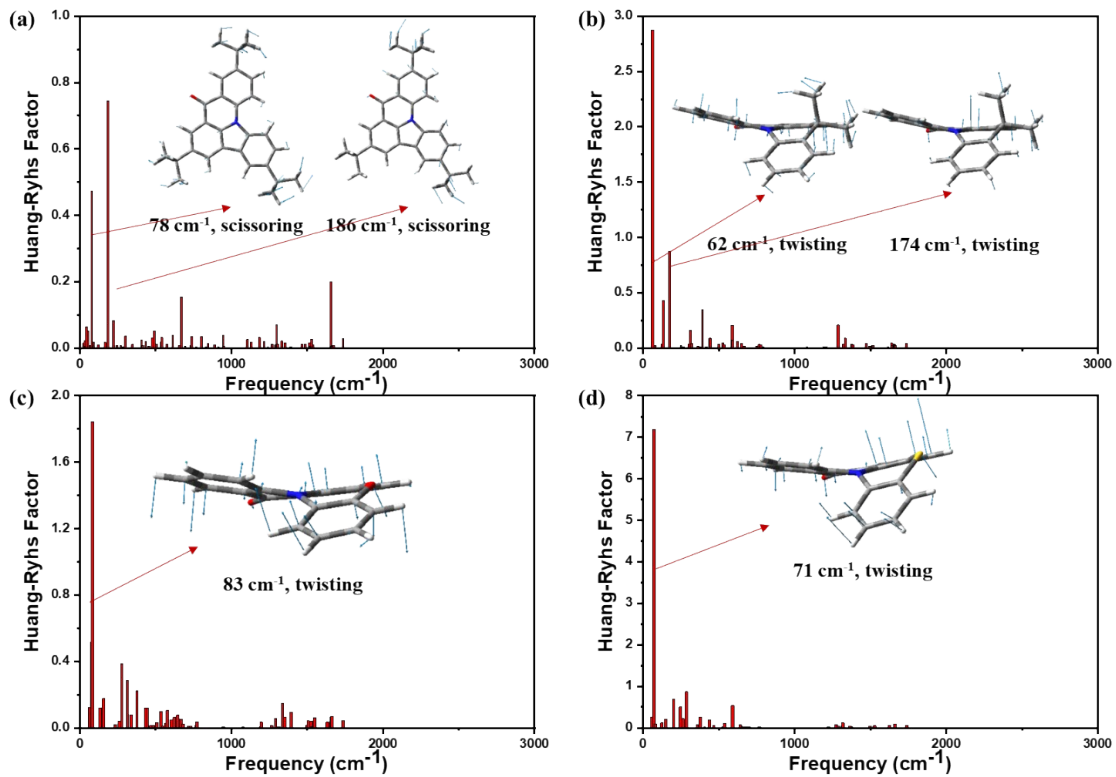


Figure S20. Huang-Ryhs factor calculated for (a) CzAO, (b) MQAO, (c) QP XO, (d) QPO optimized at B3LYP/6-31G(d) level. Vibration modes with large contributions to the Huang–Rhys factors are shown as insets.

Table S5. Cartesian coordinates for CzAO.

CzAO-S ₀ E(B3LYP) = -1332.431555 hartree							
C	-2.19254	-3.3854	-0.0043	H	-4.16312	-0.62205	0.00336
C	-3.3849	-2.64137	-0.0009	H	-0.05993	-3.44458	-0.00895
C	-3.27221	-1.24422	0.001656	H	-3.38694	1.999064	0.003833
C	-2.02327	-0.62779	0.001583	H	0.411003	4.064322	-0.00314
C	-0.83108	-1.40593	-0.00047	H	4.481004	1.190596	-0.00685
C	-0.92455	-2.79651	-0.00434	H	4.079312	-3.09484	0.01263
C	-1.62967	0.770471	0.001816	H	1.683844	-2.87296	0.014553
C	-0.2265	0.771098	0.000153	H	-4.27868	5.446908	0.004467
N	0.278777	-0.52019	3.71E-05	H	-4.19327	3.921903	-0.8839
C	-2.30269	1.992315	0.002411	H	-4.19055	3.922211	0.893083
C	-1.58587	3.205931	0.00093	H	-2.35738	6.354101	1.272682
C	-0.18104	3.15462	-0.00142	H	-0.7904	5.531683	1.302281
C	0.523567	1.944311	-0.00185	H	-2.16461	4.838188	2.17552
C	1.669598	-0.70662	0.001215	H	-0.79439	5.531313	-1.30402
C	2.510469	0.438093	-0.00293	H	-2.17095	4.83697	-2.17286
C	3.90535	0.272474	-0.00328	H	-2.36147	6.353346	-1.27033
C	4.518885	-0.97546	0.001143	H	7.878401	-0.01042	-0.0099
C	3.660277	-2.09237	0.007442	H	6.562114	0.7665	-0.89941
C	2.278687	-1.97276	0.007626	H	6.565256	0.777566	0.874341

C	1.990184	1.836258	-0.00522	H	-5.71521	-5.2555	-0.00257
C	-2.29064	4.577575	0.001579	H	-4.18873	-5.21849	-0.89264
C	-3.82553	4.449307	0.003941	H	-4.18637	-5.22132	0.883621
C	-1.87244	5.370272	1.262865	H	7.549529	-2.10627	1.278557
C	-1.87626	5.369641	-1.26136	H	5.989184	-2.93971	1.31445
C	-4.77837	-3.2979	-0.00063	H	6.187955	-1.40564	2.175624
C	6.043991	-1.17011	0.000525	H	-6.55461	-3.31035	1.273743
C	6.797916	0.172857	-0.0092	H	-5.68278	-1.77076	1.305381
C	-4.70271	-4.83649	-0.00322	H	-5.03146	-3.16807	2.173895
C	6.463533	-1.95329	1.267279	H	6.182005	-1.43455	-2.17173
C	-5.55557	-2.8576	1.262823	H	7.54663	-2.12198	-1.26913
C	6.460548	-1.96977	-1.2569	H	5.986996	-2.95716	-1.28964
C	-5.55805	-2.85346	-1.26111	H	-5.03573	-3.16097	-2.17422
O	2.734238	2.816809	-0.00892	H	-6.55713	-3.30615	-1.27156
H	-2.23428	-4.46849	-0.00728	H	-5.68531	-1.76649	-1.29988

CzAO-S ₁ E(B3LYP) = -1332.315323 hartree							
C	-2.08228	-3.42396	-0.17156	H	-4.13641	-0.7092	0.13273
C	-3.29067	-2.70103	-0.03784	H	0.047445	-3.39111	-0.34213
C	-3.22311	-1.29052	0.057331	H	-3.44806	1.985444	0.135471
C	-2.00588	-0.62941	0.044111	H	0.32883	4.105874	-0.1008
C	-0.78602	-1.39857	-0.03745	H	4.432823	1.221886	-0.22201
C	-0.84151	-2.79669	-0.18155	H	4.092943	-3.04362	0.411587
C	-1.64427	0.772845	0.06891	H	1.676776	-2.81562	0.465677
C	-0.26341	0.810304	0.009617	H	-4.36313	5.426153	0.145336
N	0.27767	-0.51889	-0.00989	H	-4.30942	3.889813	-0.72891
C	-2.36703	1.998976	0.088829	H	-4.2151	3.910651	1.044776
C	-1.65228	3.204191	0.034303	H	-2.38795	6.365584	1.295158
C	-0.24149	3.186289	-0.04414	H	-0.81498	5.550177	1.260389
C	0.497853	1.974371	-0.06187	H	-2.14075	4.863754	2.209357
C	1.664949	-0.69254	0.042252	H	-0.95313	5.520279	-1.34238
C	2.477722	0.473418	-0.09043	H	-2.3594	4.791993	-2.13043
C	3.862367	0.30891	-0.10141	H	-2.5301	6.321988	-1.24591
C	4.491159	-0.94142	0.048118	H	7.831174	0.052753	-0.21594
C	3.6615	-2.06169	0.246744	H	6.472718	0.691528	-1.15171
C	2.274802	-1.94083	0.252157	H	6.542316	0.946229	0.601653
C	1.936282	1.868456	-0.17457	H	-5.55951	-5.36256	-0.09683
C	-2.37054	4.568953	0.049825	H	-4.09337	-5.23223	-1.07265
C	-3.90246	4.4317	0.132585	H	-3.98066	-5.35772	0.696283
C	-1.89642	5.384639	1.276266	H	7.578527	-1.83411	1.363514
C	-2.02883	5.345853	-1.24411	H	6.03981	-2.68347	1.569041
C	-4.6606	-3.39098	-0.01296	H	6.232556	-1.04215	2.205795
C	6.016133	-1.10781	0.023224	H	-6.35813	-3.53534	1.350288
C	6.749777	0.228085	-0.19881	H	-5.52465	-1.9771	1.446058
C	-4.55653	-4.92354	-0.12874	H	-4.79347	-3.41332	2.178597

C	6.489571	-1.70478	1.371931	H	6.08632	-1.67144	-2.09582
C	-5.37352	-3.0539	1.321381	H	7.489694	-2.20867	-1.15241
C	6.40195	-2.07193	-1.126	H	5.94385	-3.05909	-1.00453
C	-5.51761	-2.87318	-1.19556	H	-5.04126	-3.10136	-2.15547
O	2.704584	2.843271	-0.29164	H	-6.50289	-3.3541	-1.18142
H	-2.1069	-4.50008	-0.28626	H	-5.6744	-1.79112	-1.14736

Table S6. Cartesian coordinates for MQAO.

MQAO-S ₀ E(B3LYP) = -978.5935653 hartree							
C	-3.041003	-2.579491	0.973007	H	-3.196028	-3.566694	1.400296
C	-4.143703	-1.780449	0.633652	H	-5.154357	-2.150006	0.779427
C	-3.923848	-0.508487	0.133031	H	-4.742525	0.157308	-0.120971
C	-2.620252	-0.019144	-0.055845	H	-0.904601	-2.744471	1.075574
C	0.893342	-1.202567	-0.286431	H	2.508120	3.313839	0.066803
C	-1.744150	-2.122542	0.787550	H	0.680738	4.804632	-0.640507
C	1.306068	1.538135	0.147000	H	-1.643756	3.880755	-0.891639
C	0.005617	1.027736	-0.068287	H	4.287550	-1.217972	-0.221883
N	-0.205391	-0.355872	0.062770	H	3.931564	-3.359194	-1.377681
C	1.518652	2.895215	-0.081106	H	1.608563	-4.105151	-1.912720
C	0.477940	3.750581	-0.474752	H	-0.311359	-2.706890	-1.255639
C	-0.803850	3.250081	-0.619041	C	2.361634	0.585069	0.720744
C	-1.057108	1.884970	-0.413719	C	3.785648	1.151399	0.594922
C	-1.512218	-0.841081	0.247833	H	3.873693	2.094193	1.143026
C	2.198438	-0.750485	-0.010362	H	4.515156	0.466032	1.036653
C	3.273466	-1.546679	-0.419584	H	4.066502	1.330060	-0.448505
C	3.076721	-2.758398	-1.080855	C	2.063831	0.370256	2.234297
C	1.780273	-3.179106	-1.371205	H	2.786384	-0.333312	2.663520
C	0.692699	-2.398024	-0.990181	H	2.140977	1.321345	2.773190
C	-2.435599	1.369582	-0.526782	H	1.059932	-0.031890	2.396276
O	-3.373050	2.064884	-0.918490				

MQAO-S ₁ E(B3LYP) = -978.4780326 hartree							
C	-3.099666	-2.45283	1.140721	H	-3.27764	-3.40353	1.632994
C	-4.154816	-1.67964	0.668515	H	-5.17731	-2.03073	0.782831
C	-3.916147	-0.44018	0.055684	H	-4.72781	0.185175	-0.30022
C	-2.610429	0.043075	-0.11095	H	-0.9407	-2.57903	1.334656
C	0.805771	-1.1962	-0.32821	H	2.590209	3.314778	0.26077
C	-1.775365	-1.99324	0.962624	H	0.790553	4.817546	-0.48429
C	1.345824	1.528132	0.245728	H	-1.50817	3.920097	-0.93545
C	0.057569	1.07319	0.000419	H	4.208926	-1.34756	-0.36826
N	-0.212062	-0.34165	0.024067	H	3.723753	-3.48247	-1.47621
C	1.599015	2.915172	0.086338	H	1.362829	-4.18907	-1.87416
C	0.579342	3.761195	-0.33724	H	-0.49138	-2.72045	-1.1574
C	-0.708951	3.27577	-0.58603	C	2.404501	0.513039	0.677782
C	-1.003863	1.916143	-0.40379	C	3.836278	1.043795	0.479475

C	-1.546103	-0.79384	0.300136	H	3.985529	1.953534	1.066446
C	2.158208	-0.77636	-0.10475	H	4.576277	0.320535	0.835217
C	3.17458	-1.62795	-0.528	H	4.046219	1.272847	-0.57033
C	2.902474	-2.85013	-1.15261	C	2.215734	0.204041	2.198535
C	1.576019	-3.2532	-1.36697	H	2.949493	-0.5378	2.534705
C	0.535611	-2.44289	-0.95846	H	2.354054	1.12203	2.77894
C	-2.362011	1.401058	-0.62143	H	1.213285	-0.18014	2.408172
O	-3.284389	2.118354	-1.06775				

Table S7. Cartesian coordinates for **QPXO**.

QPXO-S ₀ E(B3LYP) = -935.8639512 hartree							
C	2.014993	-3.23887	-0.70385	C	-1.81316	-1.95802	0.687609
C	3.271266	-2.73681	-0.33162	C	-3.14626	-2.33969	0.848727
C	3.375336	-1.41365	0.061112	C	-4.17746	-1.49607	0.4384
C	2.245157	-0.58026	0.11895	C	-3.87102	-0.24641	-0.10043
C	-1.49122	-0.73851	0.080455	O	3.513515	1.302282	0.834185
C	0.880284	-2.44297	-0.64529	H	1.921857	-4.26184	-1.05871
O	-2.28652	1.389434	-0.75926	H	4.15108	-3.37167	-0.37495
C	-1.07768	1.94412	-0.38461	H	4.329074	-0.96732	0.324028
C	0.019689	1.115117	-0.09144	H	-0.07244	-2.84139	-0.97143
N	-0.15788	-0.27644	-0.133	H	-1.82597	3.924689	-0.59792
C	-0.95611	3.321897	-0.35737	H	0.373542	4.98872	-0.03149
C	0.281853	3.906957	-0.04378	H	2.349155	3.522432	0.471289
C	1.375553	3.10584	0.236956	H	-1.02195	-2.60961	1.037182
C	1.257433	1.704279	0.212272	H	-3.37046	-3.29869	1.305994
C	2.435433	0.848202	0.452144	H	-5.21482	-1.79366	0.55701
C	-2.54256	0.126917	-0.26423	H	-4.6437	0.457769	-0.39153
C	0.970768	-1.10674	-0.20367				

QPXO-S ₁ E(B3LYP) = -935.7567011 hartree							
C	2.057236	-3.20571	-0.82684	C	-1.76702	-2.0239	0.631304
C	3.265441	-2.72549	-0.33674	C	-3.08542	-2.42278	0.773194
C	3.366087	-1.41938	0.155674	C	-4.1458	-1.56529	0.426422
C	2.24391	-0.56802	0.192787	C	-3.87147	-0.28426	-0.03102
C	-1.45413	-0.73682	0.137501	O	3.487186	1.341463	0.915603
C	0.909694	-2.37447	-0.77677	H	1.973427	-4.20994	-1.22969
O	-2.3452	1.410627	-0.58803	H	4.147107	-3.36171	-0.34897
C	-1.09144	1.954466	-0.40411	H	4.309326	-1.01061	0.500689
C	-0.00299	1.137955	-0.12165	H	-0.0326	-2.73961	-1.16945
N	-0.17105	-0.2668	-0.05945	H	-1.86146	3.948612	-0.67585
C	-0.9819	3.354548	-0.45512	H	0.371316	4.994212	-0.17802
C	0.254638	3.914618	-0.16843	H	2.313166	3.526618	0.428756
C	1.352319	3.098337	0.162785	H	-0.96026	-2.688	0.910516
C	1.249948	1.705031	0.18472	H	-3.29816	-3.41315	1.16374
C	2.406047	0.849264	0.521306	H	-5.17419	-1.89542	0.530878

C	-2.5478	0.136641	-0.15554	H	-4.65819	0.418066	-0.28515
C	0.997976	-1.11111	-0.21813				

Table S8. Cartesian coordinates for QPO.

QPO-S ₀ E(B3LYP) = -1258.836432 hartree							
C	-2.30072	-3.04874	0.970163	C	3.722247	-2.11652	-0.8752
C	-3.52694	-2.50306	0.558464	C	2.51214	-2.67397	-1.29053
C	-3.55502	-1.21581	0.050182	C	1.304365	-2.06539	-0.95623
C	-2.37602	-0.46001	-0.07091	C	-2.46071	0.932027	-0.55892
C	1.283486	-0.91065	-0.16061	O	-3.49245	1.408286	-1.02989
C	-1.1228	-2.32542	0.852924	H	-2.26694	-4.04625	1.400006
S	2.5027	1.191652	1.139185	H	-4.44237	-3.07942	0.65298
C	1.070948	1.93175	0.376738	H	-4.48033	-0.74283	-0.2629
C	-0.04237	1.123559	0.068585	H	-0.1858	-2.75294	1.191341
N	0.048964	-0.27637	0.201015	H	1.877098	3.914829	0.428779
C	1.005286	3.309764	0.197	H	-0.21846	4.992081	-0.37574
C	-0.17785	3.914293	-0.25028	H	-2.2338	3.561884	-0.83091
C	-1.291	3.13197	-0.5093	H	4.6469	-0.45446	0.145168
C	-1.23788	1.736964	-0.35322	H	4.665461	-2.58622	-1.13781
C	-1.14064	-1.02398	0.314241	H	2.502464	-3.57743	-1.8933
C	2.505139	-0.32973	0.215087	H	0.371002	-2.49185	-1.30512
C	3.714736	-0.92963	-0.14609				

QPO-S ₁ E(B3LYP) = -1258.730863 hartree							
C	2.378326	-2.95557	-1.13905	C	-3.67529	-2.23375	0.821406
C	3.544379	-2.45986	-0.55922	C	-2.43504	-2.83666	1.109936
C	3.548337	-1.21856	0.080873	C	-1.24601	-2.20522	0.803243
C	2.371718	-0.4509	0.177556	C	2.409598	0.925626	0.671842
C	-1.23635	-0.92408	0.19472	O	3.427747	1.439607	1.191507
C	1.184024	-2.20962	-1.03499	H	2.37224	-3.91058	-1.65485
S	-2.62234	1.233206	-0.88728	H	4.464607	-3.03605	-0.61695
C	-1.06747	1.944164	-0.46151	H	4.453106	-0.79712	0.505531
C	0.019265	1.141689	-0.124	H	0.266964	-2.59028	-1.47377
N	-0.0565	-0.27933	-0.12163	H	-1.86117	3.95579	-0.65352
C	-0.99418	3.35629	-0.39575	H	0.252425	5.01451	0.149549
C	0.181235	3.93444	0.058957	H	2.187268	3.562471	0.812328
C	1.27091	3.130015	0.423457	H	-4.64419	-0.48765	0.026127
C	1.226976	1.735593	0.324889	H	-4.60331	-2.74065	1.065201
C	1.179255	-1.01395	-0.33566	H	-2.40704	-3.80864	1.593402
C	-2.50193	-0.31096	-0.06978	H	-0.30077	-2.67487	1.041081
C	-3.69929	-0.97865	0.240008				

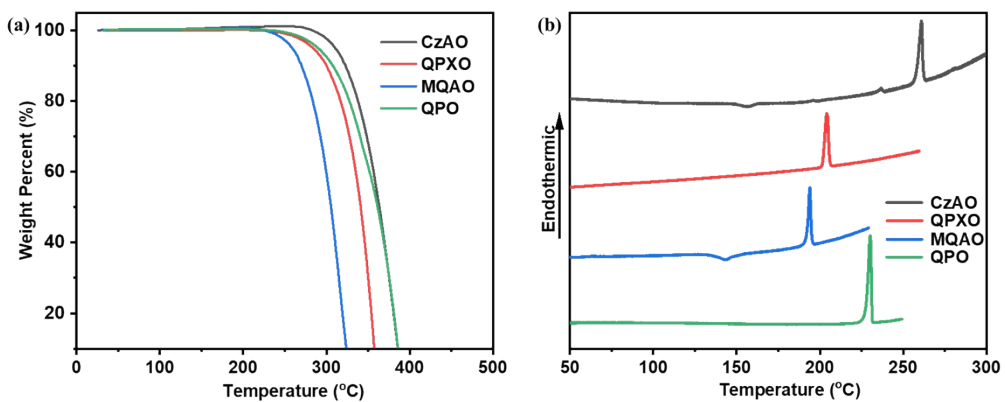


Figure S21. (a) TGA and (b) DSC curves of CzAO, MQAO, QP XO and QPO

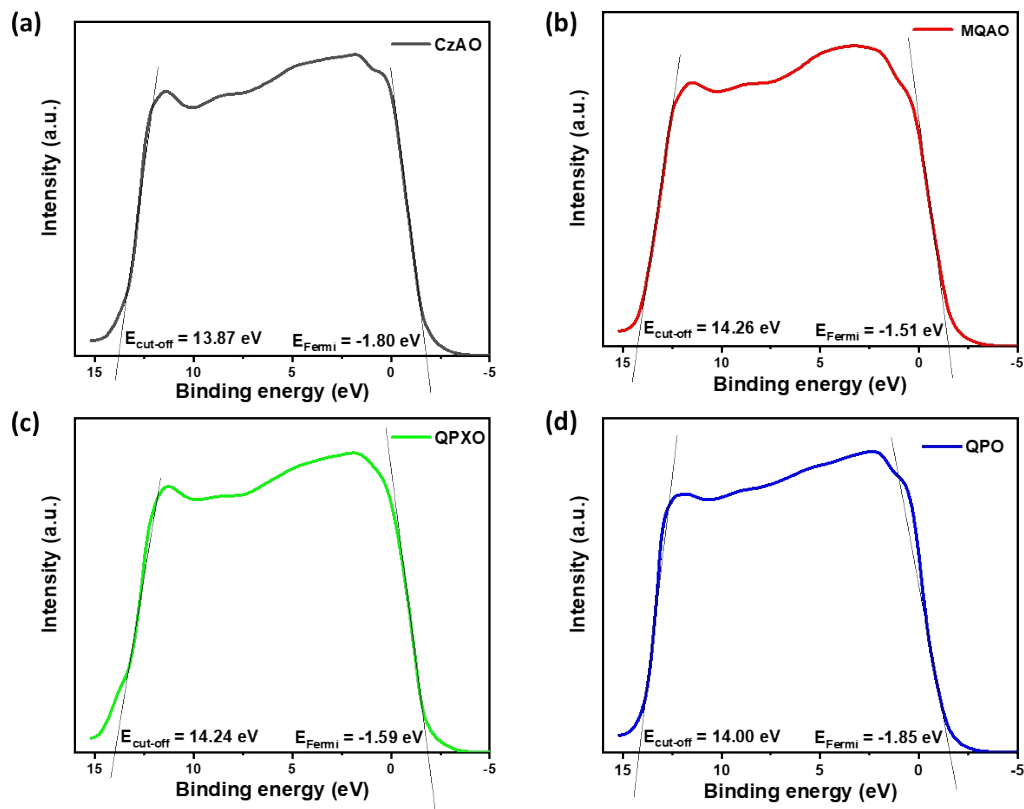


Figure S22. Ultraviolet photoelectron spectroscopy (UPS) of (a) CzAO (b) MQAO (c) QP XO and (d) QPO. $E_{\text{cut-off}}$ means the energy of cut-off region and E_{Fermi} means the energy of valence band maximum.

Table S9. Relevant information derived from the UPS spectrum

Compound	E _{cut-off} (eV)	E _{Fermi} (eV)	Ionization potential (IP) ^a (eV)	HOMO ^b (eV)
CzAO	13.87	-1.80	5.55	-5.55
MQAO	14.26	-1.51	5.45	-5.45
QPXO	14.24	-1.59	5.39	-5.39
QPO	14.00	-1.85	5.37	-5.37

^a Calculated according to the equation IP = 21.22 – (E_{cut-off} - E_{Fermi}) ^b HOMO ≈ -IP

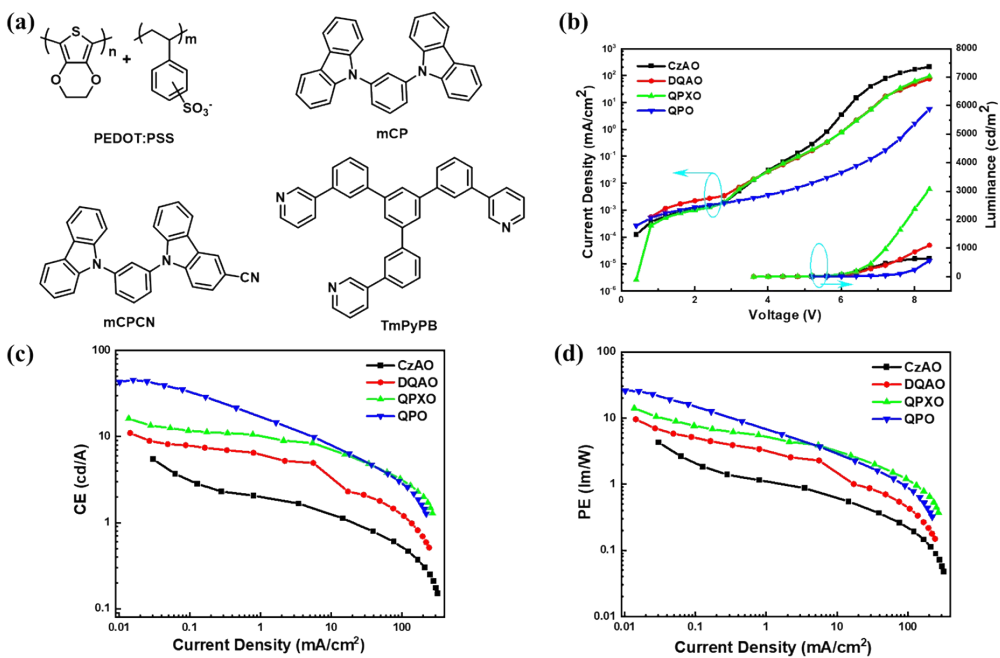


Figure S23. (a) molecular structures of materials utilized in device fabrication. (b) Current density–voltage–luminance (J – V – L) characteristics (c) Current-efficiency–luminance characteristics and f) Power-efficiency–luminance characteristics

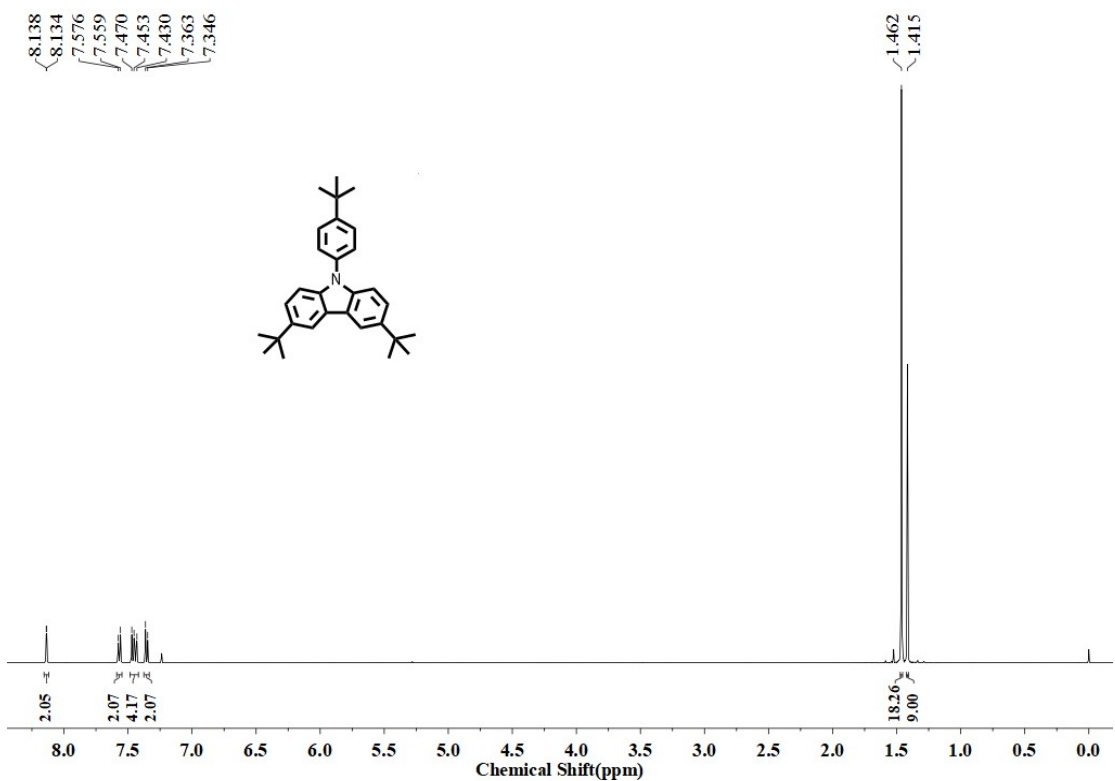


Figure 24. ¹H NMR of compound 1

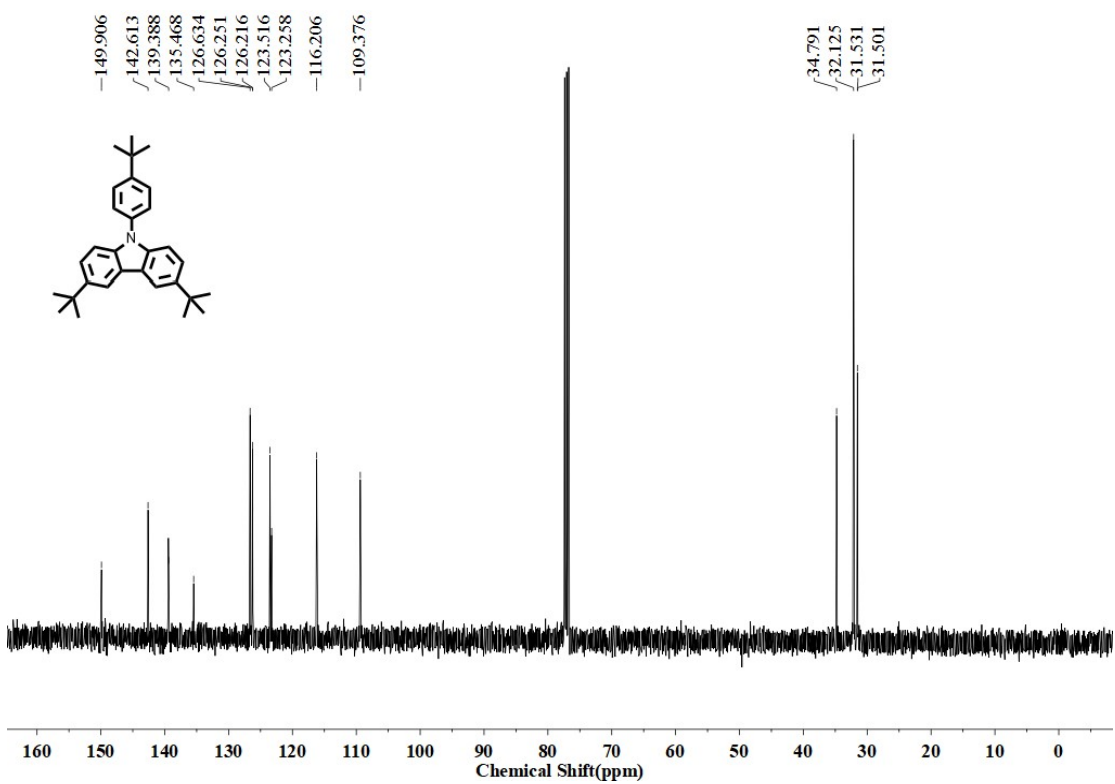


Figure 25. ¹³C NMR of compound 1

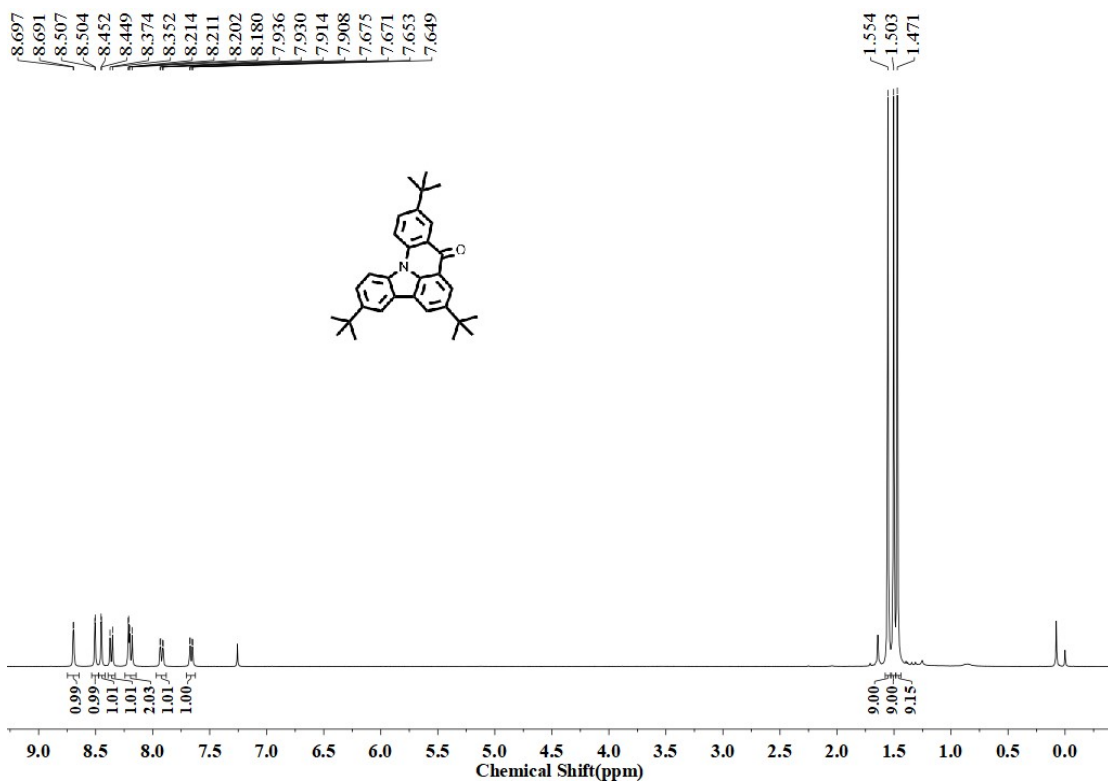


Figure 26. ^1H NMR of CzAO

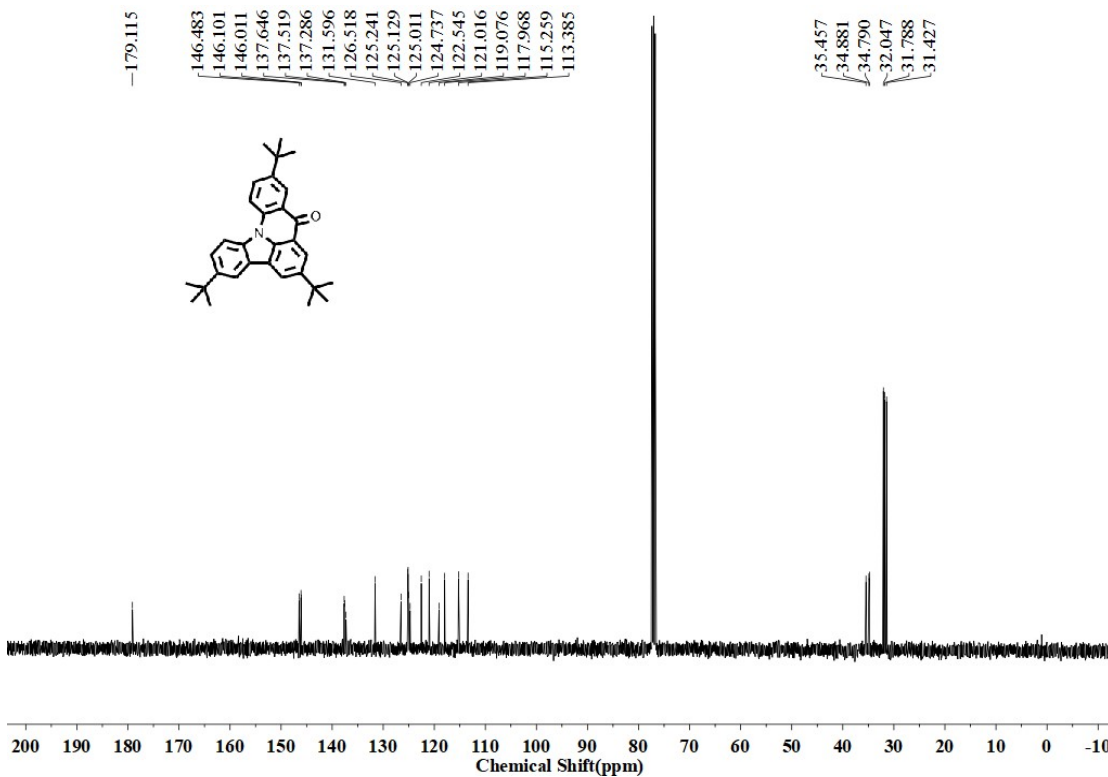


Figure 27. ^{13}C NMR of CzAO

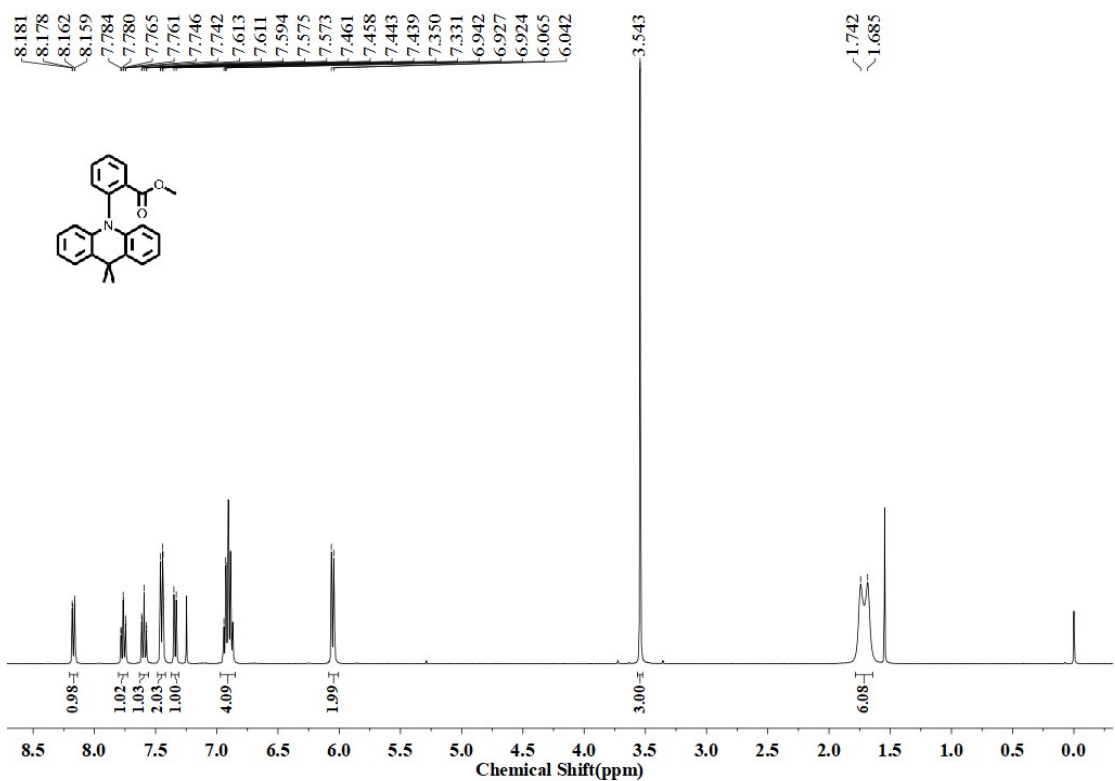


Figure 28. ¹H NMR of compound 2

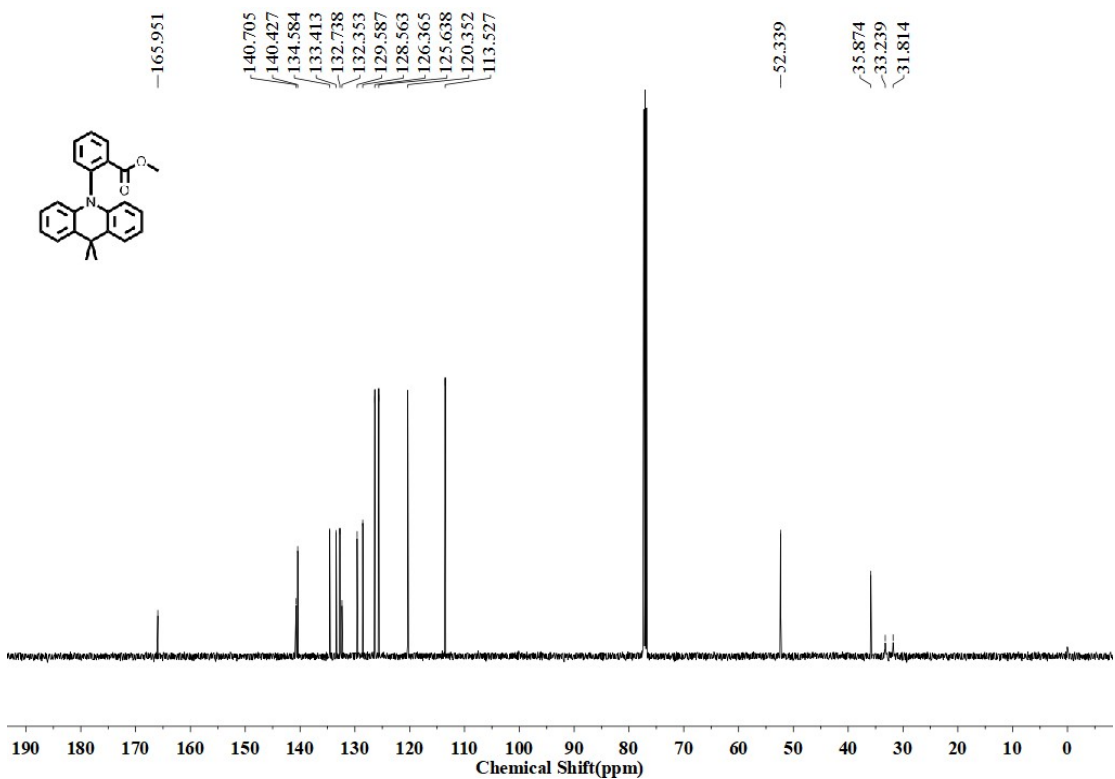


Figure 29. ¹³C NMR of compound 2

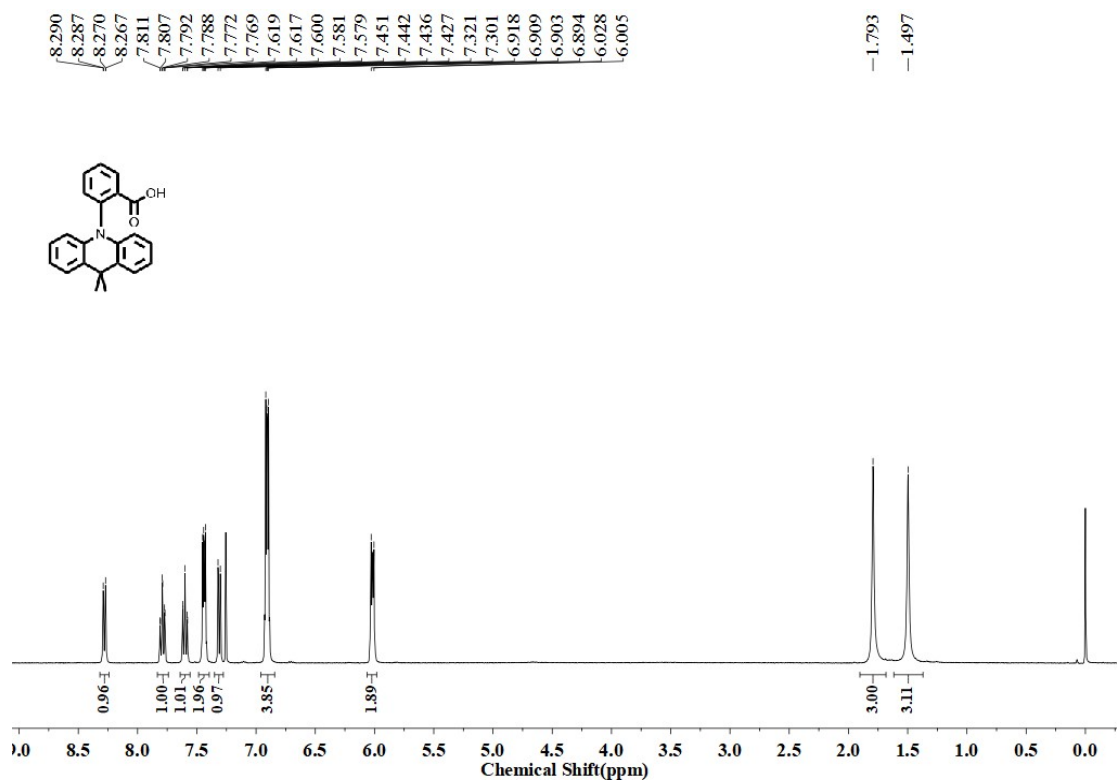


Figure 30. ¹H NMR of compound 3

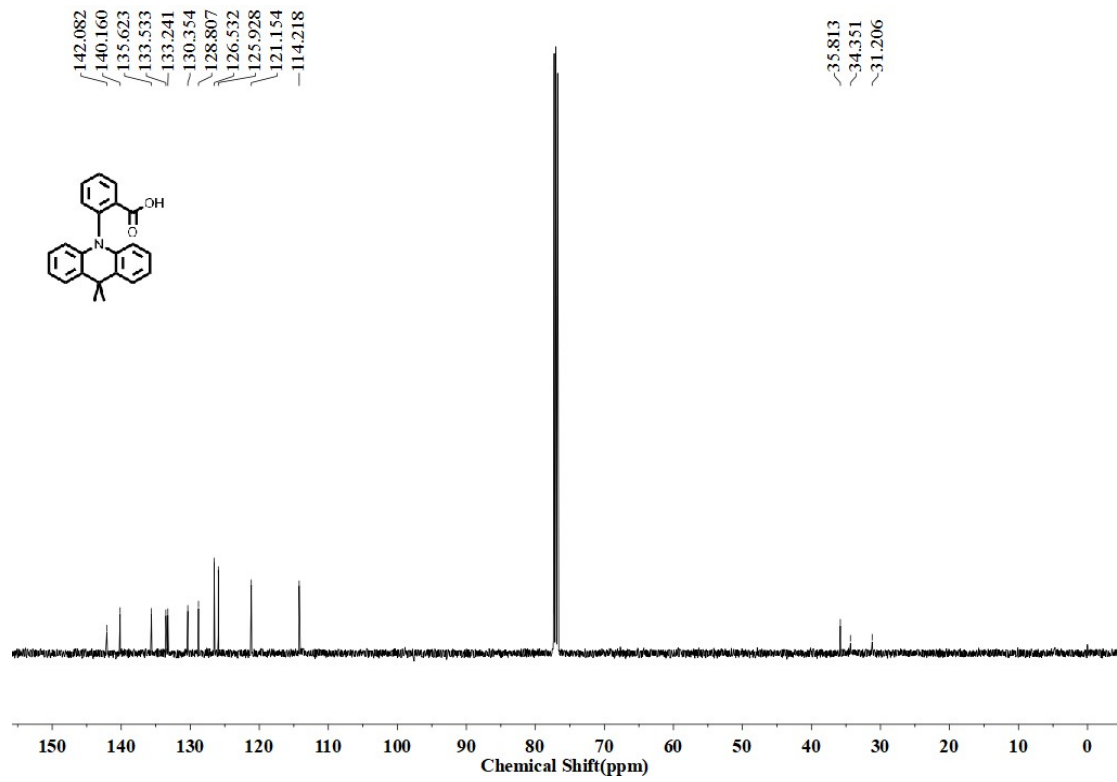


Figure 31. ¹³C NMR of compound 3

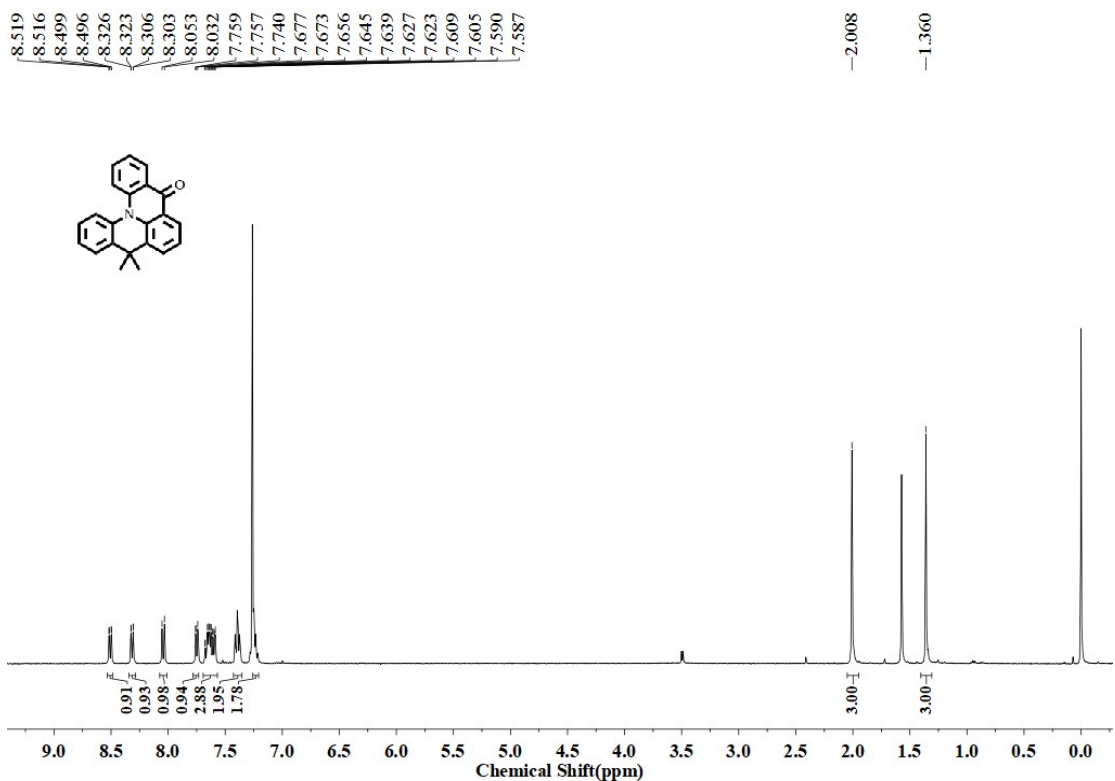


Figure 32. ¹H NMR of MQAO

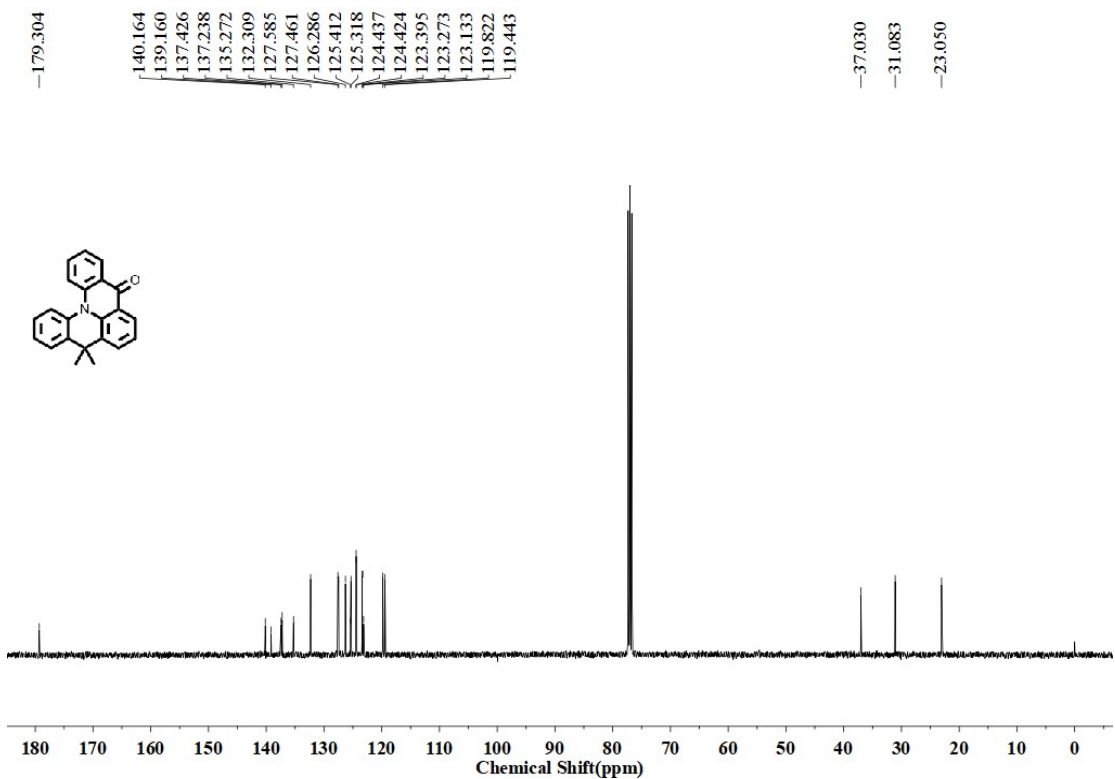


Figure 33. ¹³C NMR of MQAO

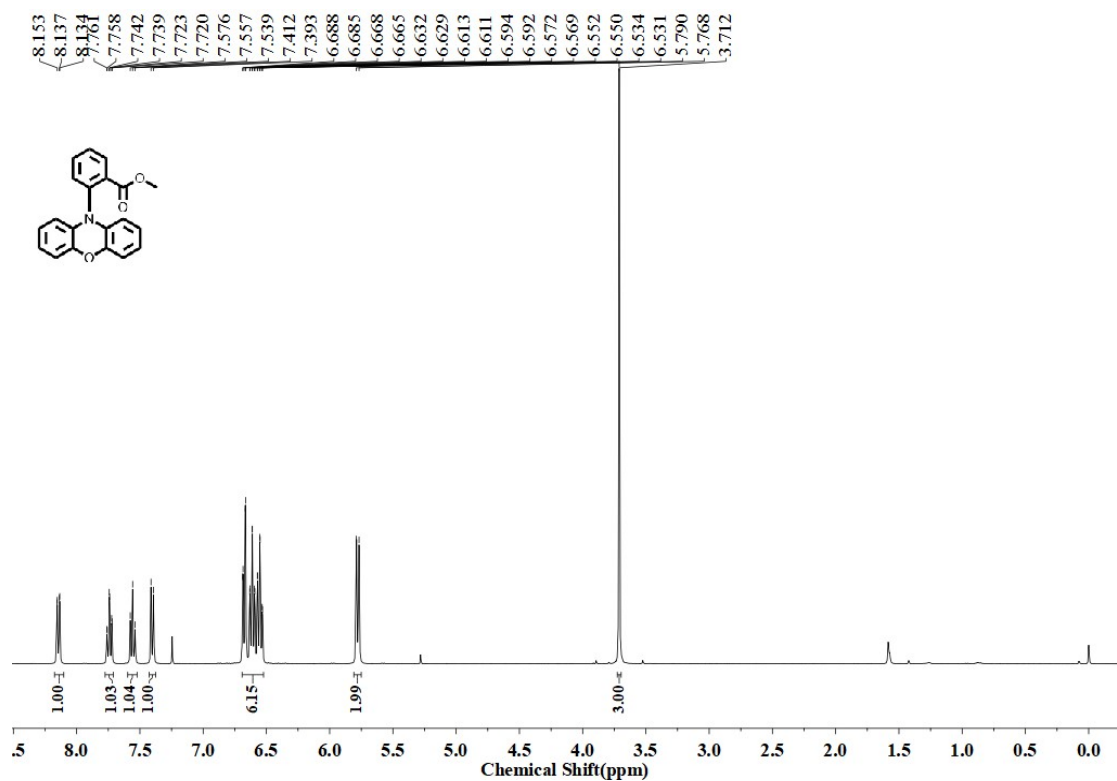


Figure 34. ¹H NMR of compound 4

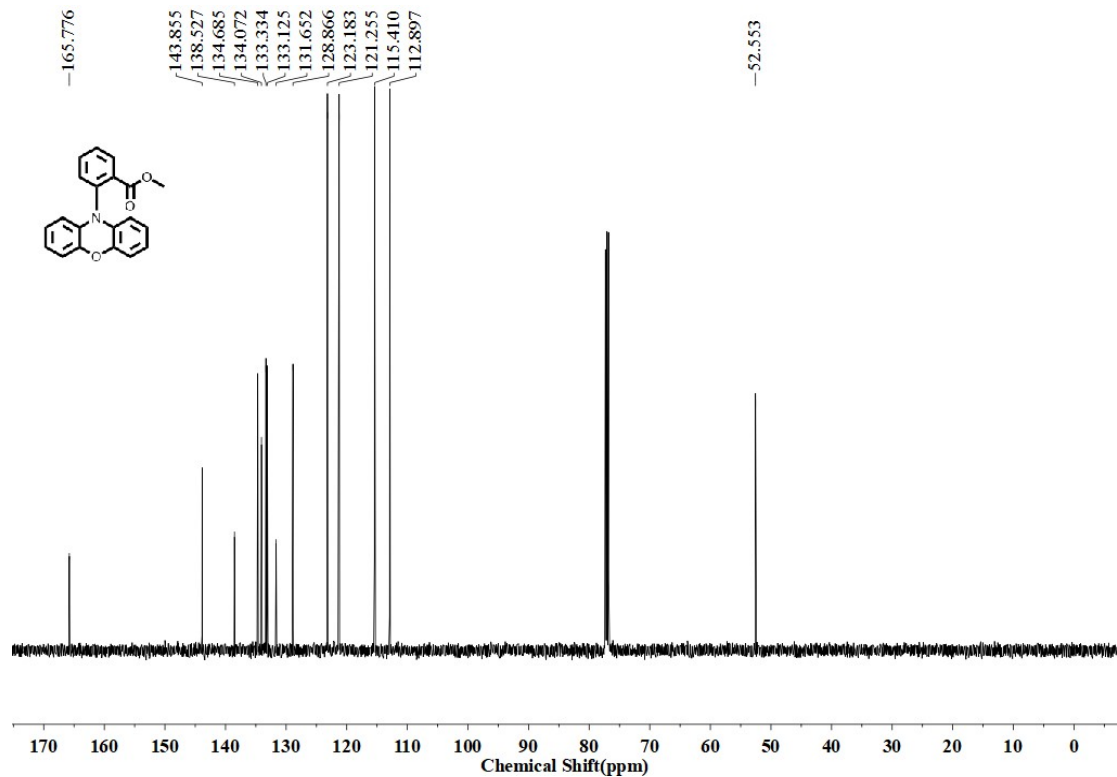


Figure 35. ¹³C NMR of compound 5

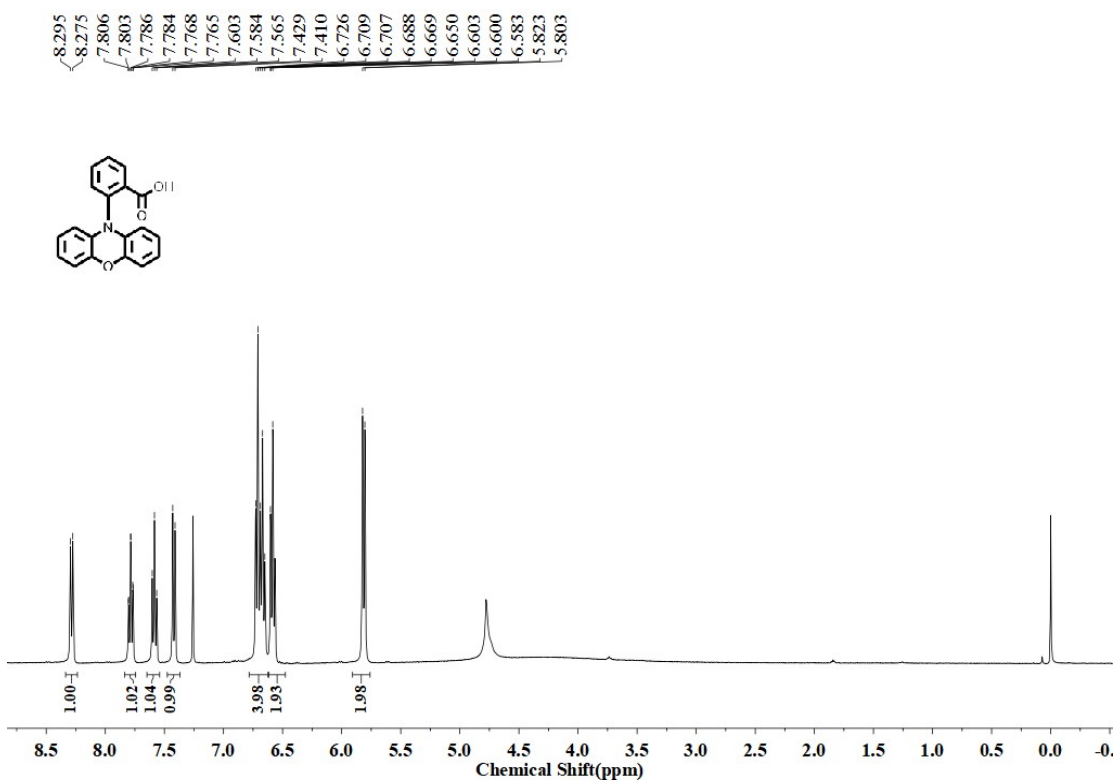


Figure 36. ^1H NMR of compound 6

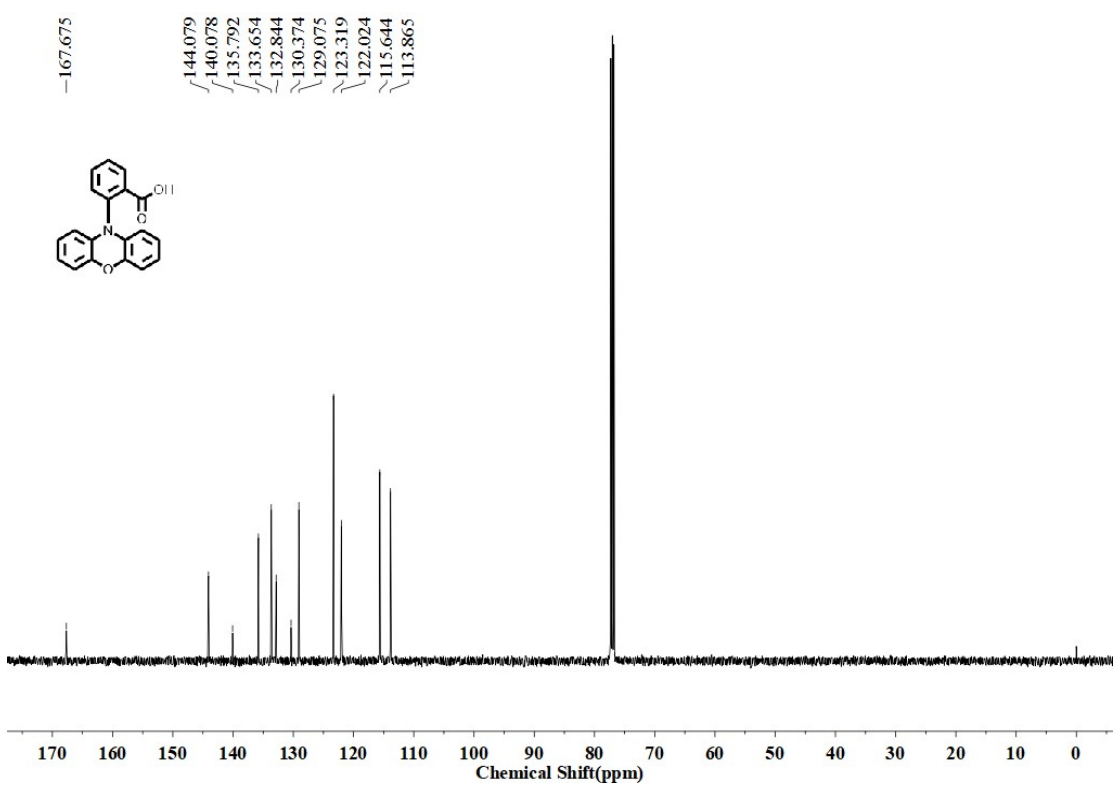


Figure 37. ^{13}C NMR of compound 6

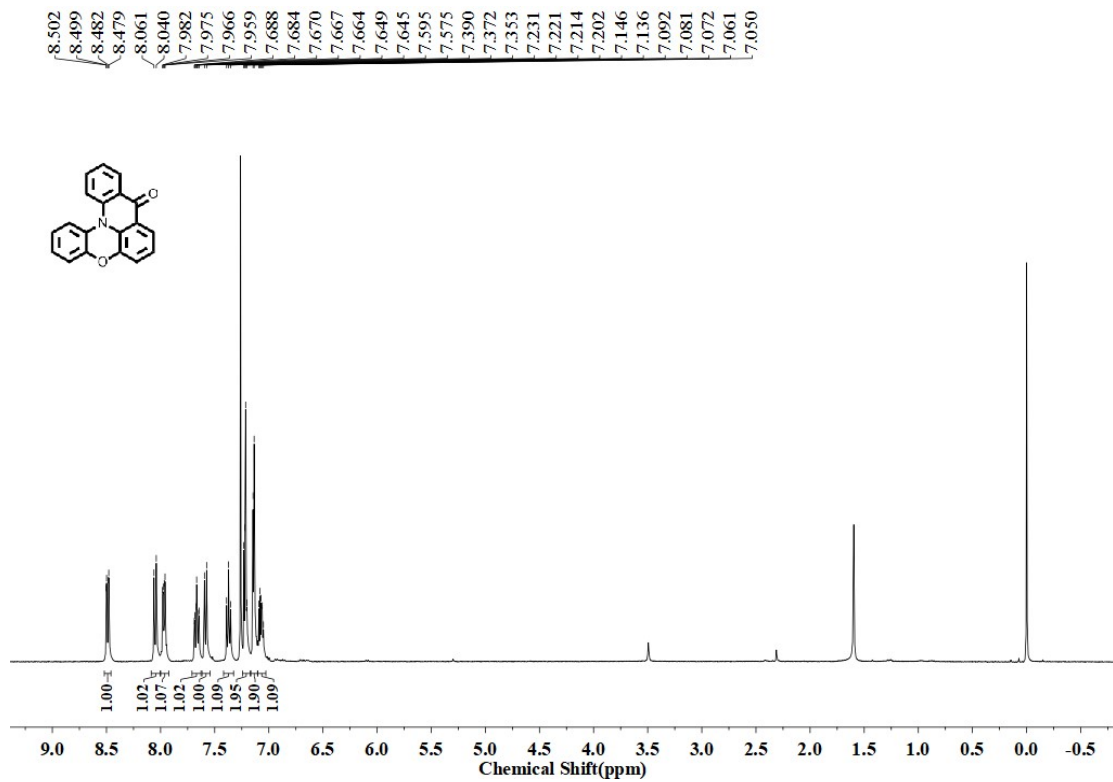


Figure 38. ^1H NMR of QP XO

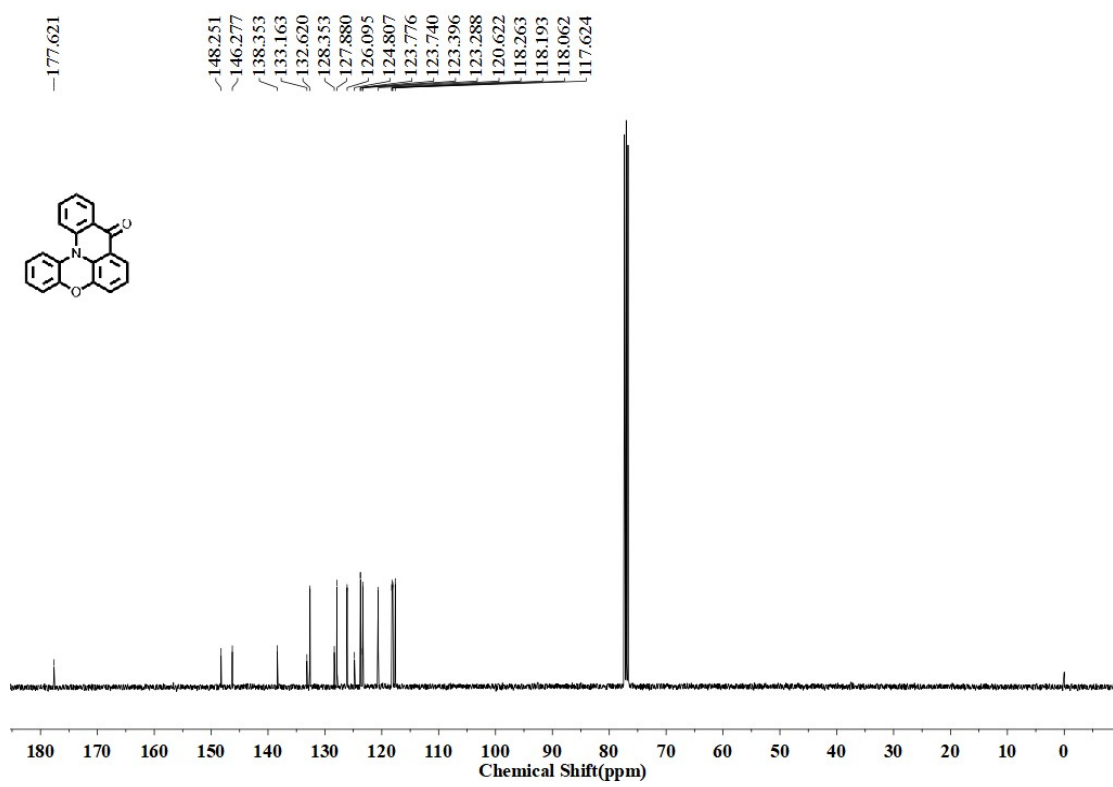


Figure 39. ^{13}C NMR of QP XO

1. X. Wu, B.-K. Su, D.-G. Chen, D. Liu, C.-C. Wu, Z.-X. Huang, T.-C. Lin, C.-H. Wu, M. Zhu, E. Y. Li, W.-Y. Hung, W. Zhu and P.-T. Chou, *Nat. Photonics*, 2021, **15**, 780-786.
2. T. Hatakeyama, K. Shiren, K. Nakajima, S. Nomura, S. Nakatsuka, K. Kinoshita, J. Ni, Y. Ono and T. Ikuta, *Adv. Mater.*, 2016, **28**, 2777-2781.
3. X. Wu, J. W. Huang, B. K. Su, S. Wang, L. Yuan, W. Q. Zheng, H. Zhang, Y. X. Zheng, W. Zhu and P. T. Chou, *Adv. Mater.*, 2022, **34**, 2105080.
4. S. N. Zou, C. C. Peng, S. Y. Yang, Y. K. Qu, Y. J. Yu, X. Chen, Z. Q. Jiang and L. S. Liao, *Org. Lett.*, 2021, **23**, 958-962.